SUPPORTING INFORMATION

2-Arylpropionic Acid Pyrazolamides as Cannabinoid CB2 Receptor Inverse Agonists Endowed with Anti-inflammatory Properties

Daniela R. de Oliveira [2], Rodolfo C. Maia [1], Patrícia R. de Carvalho [2,3], Patrícia D. Fernandes [2,3], Gisele Barbosa [1,2], Lídia M. Lima [1,2] and Carlos A. Manssour Fraga [1,2,*]

[1] Laboratório de Avaliação e Síntese de Substâncias Bioativas, Instituto de Ciências Biomédicas, Universidade Federal do Rio de Janeiro, Rio de Janeiro, RJ, 21920-190, Brazil
[2] Programa de Pós-Graduação em Farmacologia e Química Medicinal, Instituto de Ciências Biomédicas, Universidade Federal do Rio de Janeiro, Rio de Janeiro, RJ, 21920-190, Brazil
[3] Laboratório da Dor e Inflamação, Instituto de Ciências Biomédicas, Universidade Federal do Rio de Janeiro, Rio de Janeiro, RJ, 21920-190, Brazil
* Correspondence: cmfraga@ccsdecania.ufrj.br

CONTENT:

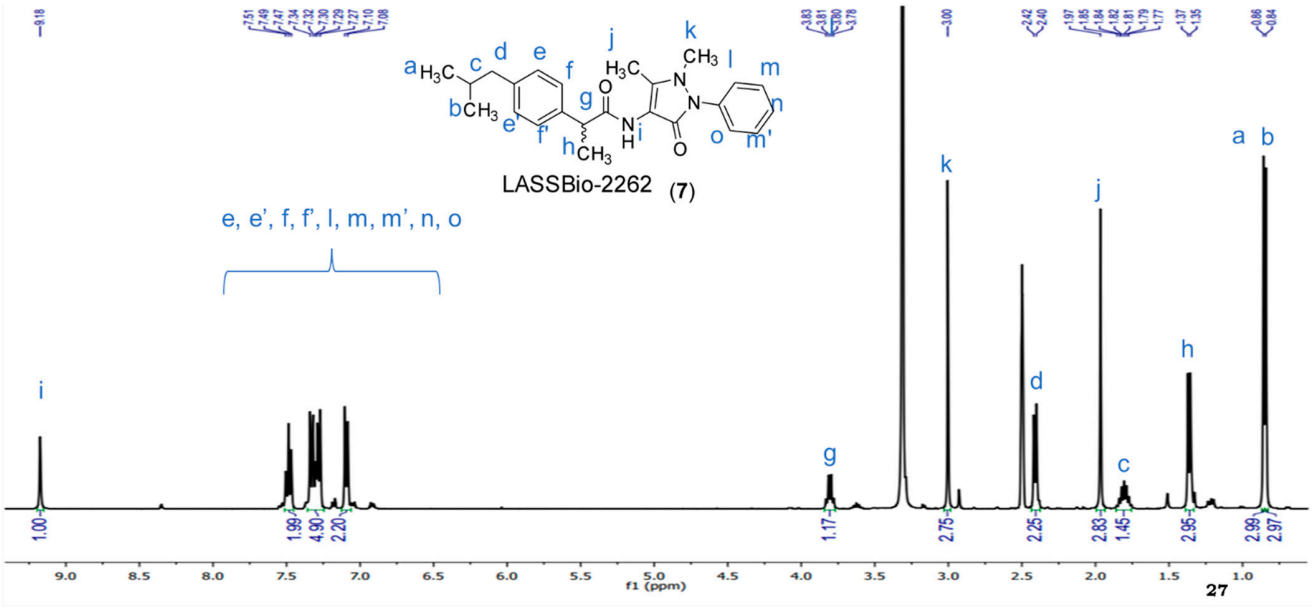

Figure S1. NMR spectrum^{1}H pyrazolamide **(7)** (400 MHz, DMSO-d6).

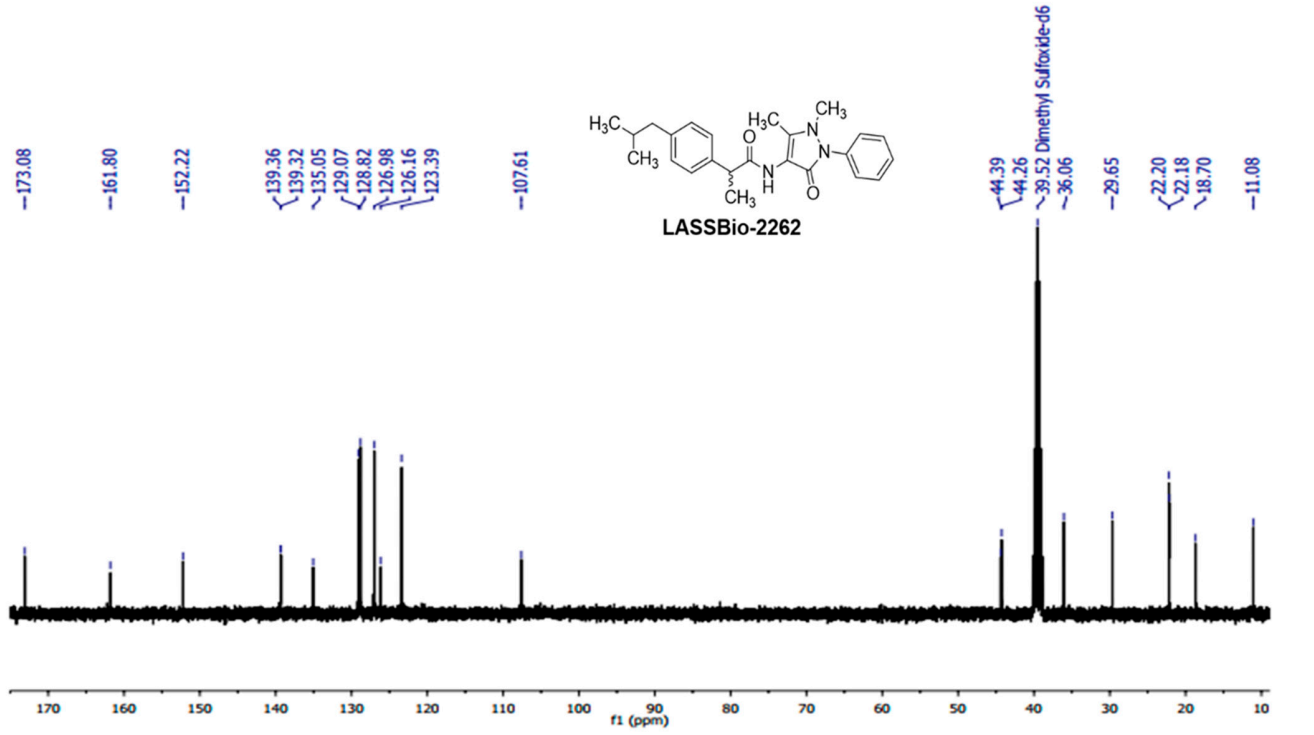

Figure S2. NMR spectrum^{13}C pyrazolamide **(7)** (50 MHz, DMSO-d6).

<Chromatogram>

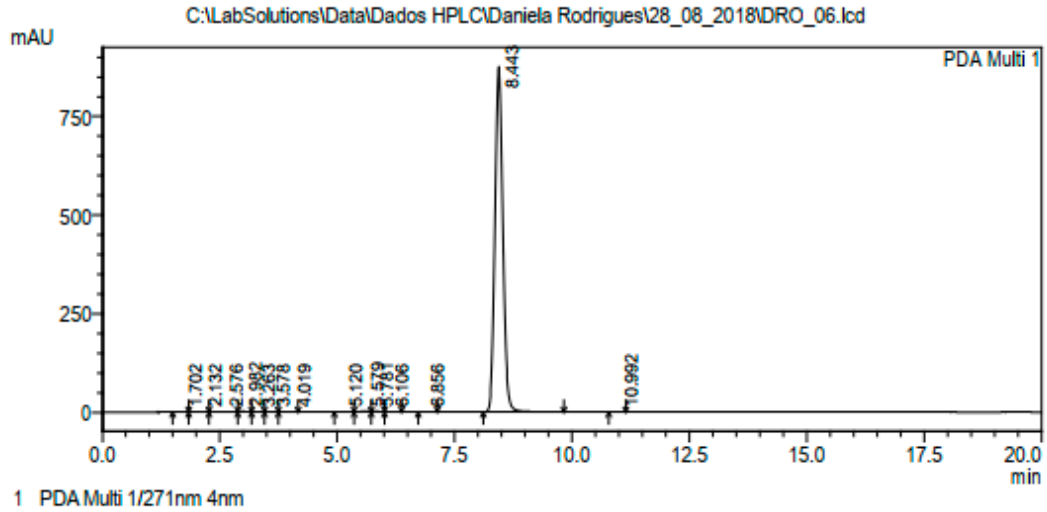

PeakTable

PDA Ch1 271nm 4nm

Peak#	Ret. Time	Area	Height	Area %	Height %
1	1.702	2255	242	0.022	0.027
2	2.132	5585	381	0.053	0.043
3	2.576	23552	995	0.225	0.112
4	2.982	14976	1971	0.143	0.222
5	3.263	5984	618	0.057	0.070
6	3.578	6686	763	0.064	0.086
7	4.019	6444	594	0.062	0.067
8	5.120	6749	742	0.065	0.084
9	5.579	30122	2219	0.288	0.250
10	5.781	20791	1824	0.199	0.206
11	6.106	7340	705	0.070	0.079
12	6.856	1699	169	0.016	0.019
13	8.443	10316978	875693	98.709	98.712
14	10.992	2705	203	0.026	0.023
Total		10451867	887119	100.000	100.000

Figure S3. Chromatogram obtained for pyrazolamide **(7)**. Conditions: Shimadzu – LC20AD; Column: Kromasil 100-5 C18 250-4.6 mm; Mobile phase: 60% ACN, 40% water; Flow: 1mL/min; Detector: SPD-M20A (Diode Array); Wavelength: 271 nm.

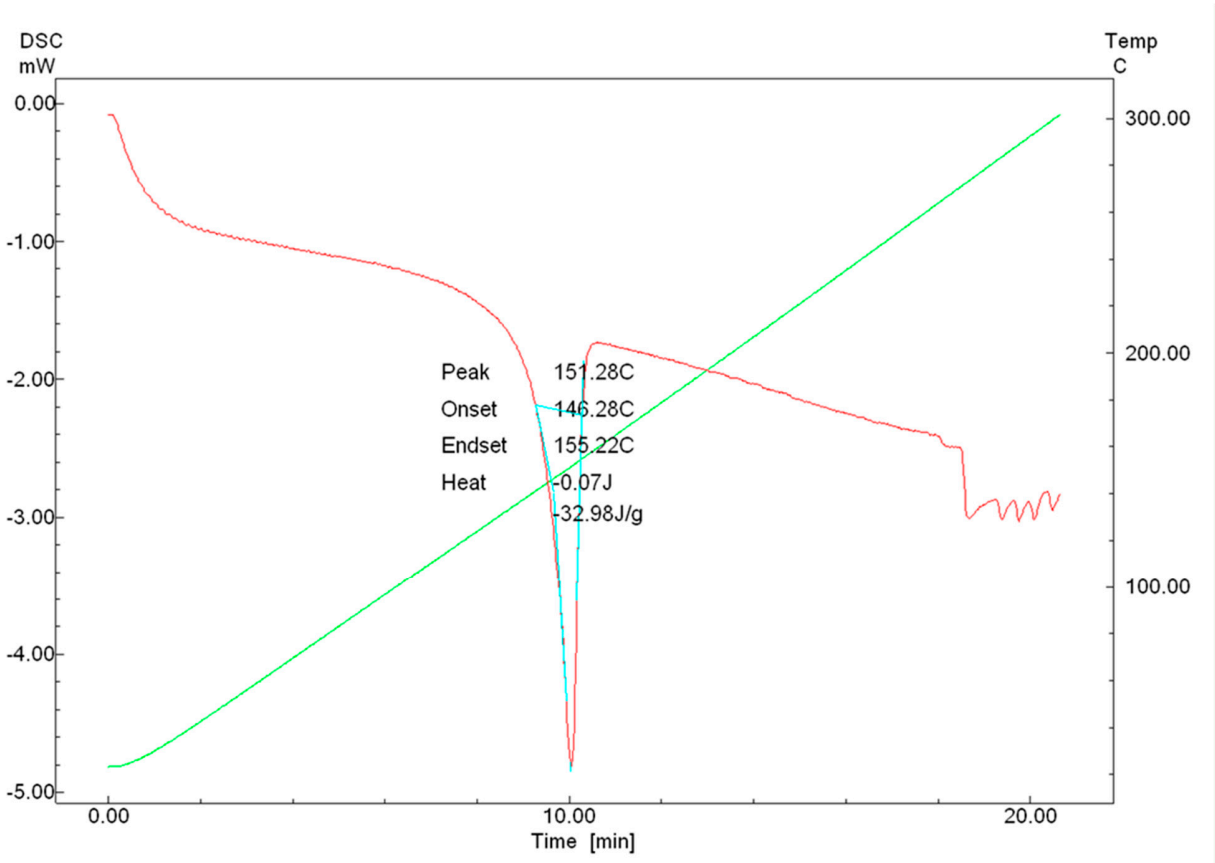

Figure S4. Determination of the melting point (FP) of pyrazolamide (**7**) determined by *Differential Scanning Calorimetry* (DSC) performed in a Shimadzu equipment (Model DSC-60).

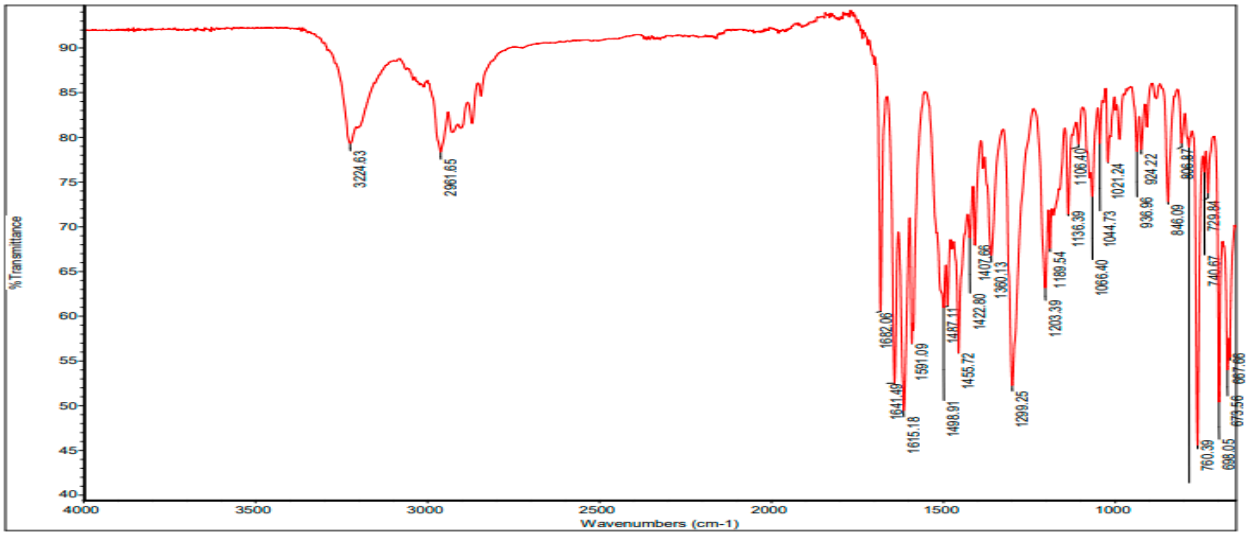

Figure S5. Infrared (ATR) of pyrazolamide (**7**).

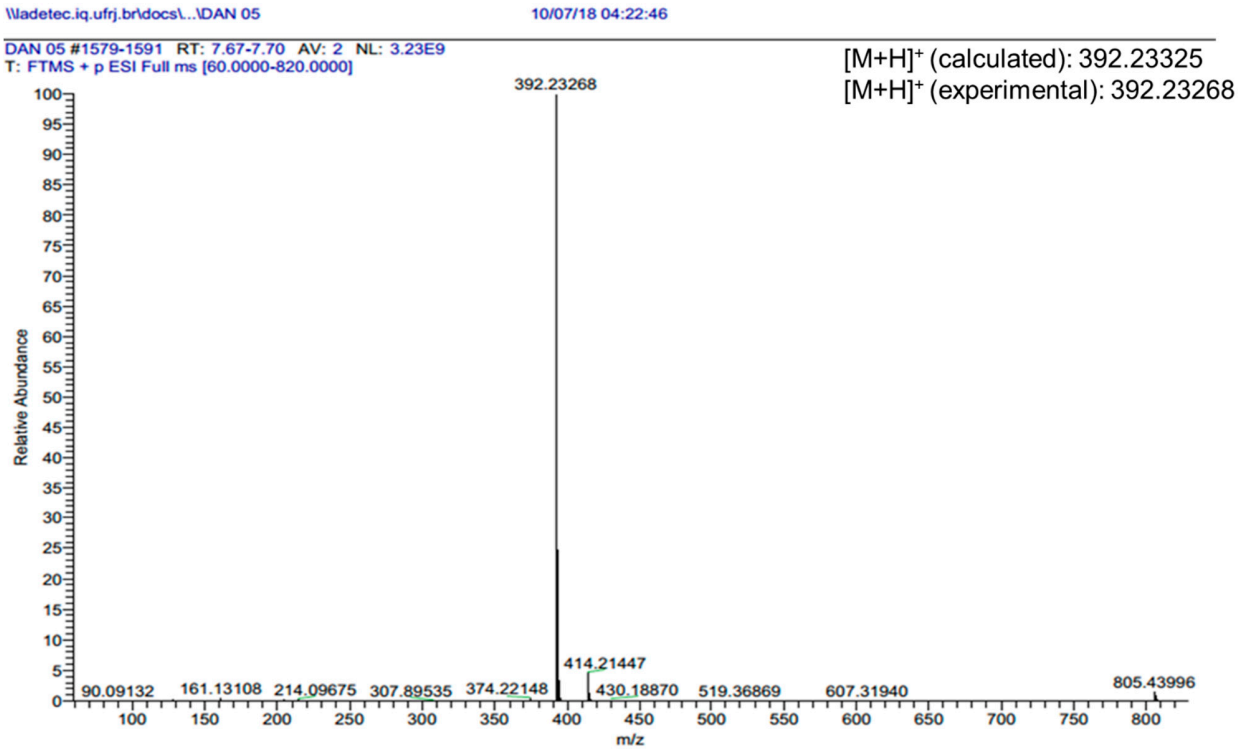

Figure S6. High resolution mass spectrum of pyrazolamide (**7**). Detection in positive mode ([M+H]+).

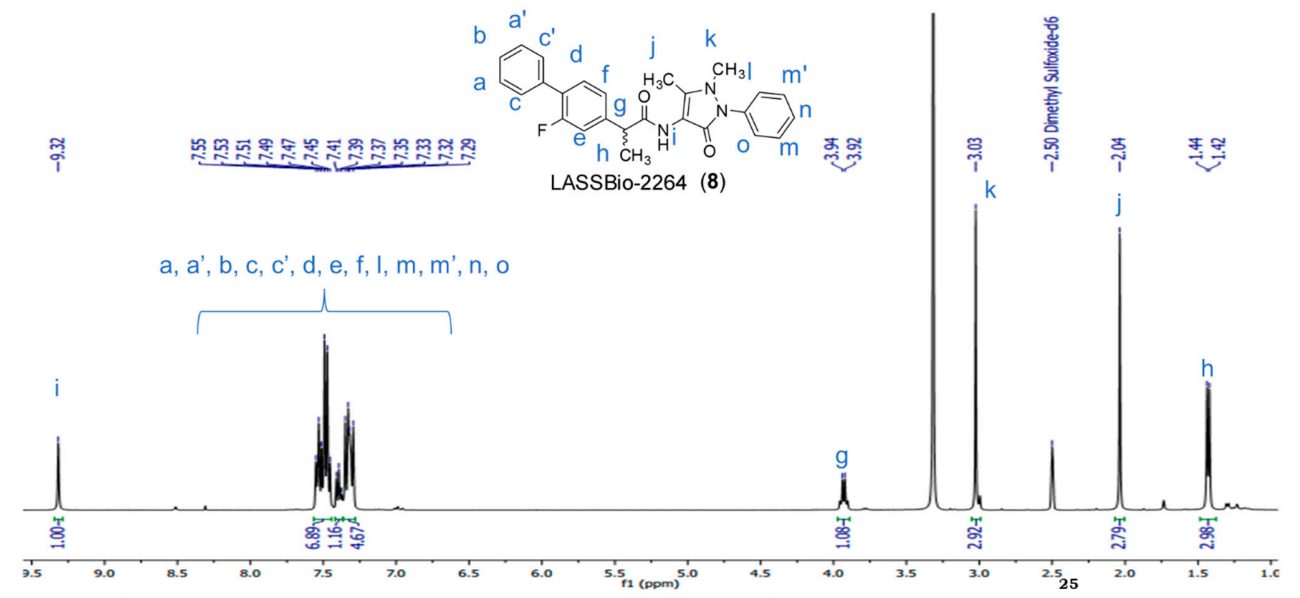

Figure S7. 1H NMR spectrum of pyrazolamide (**8**) (400 MHz, DMSO-d6).

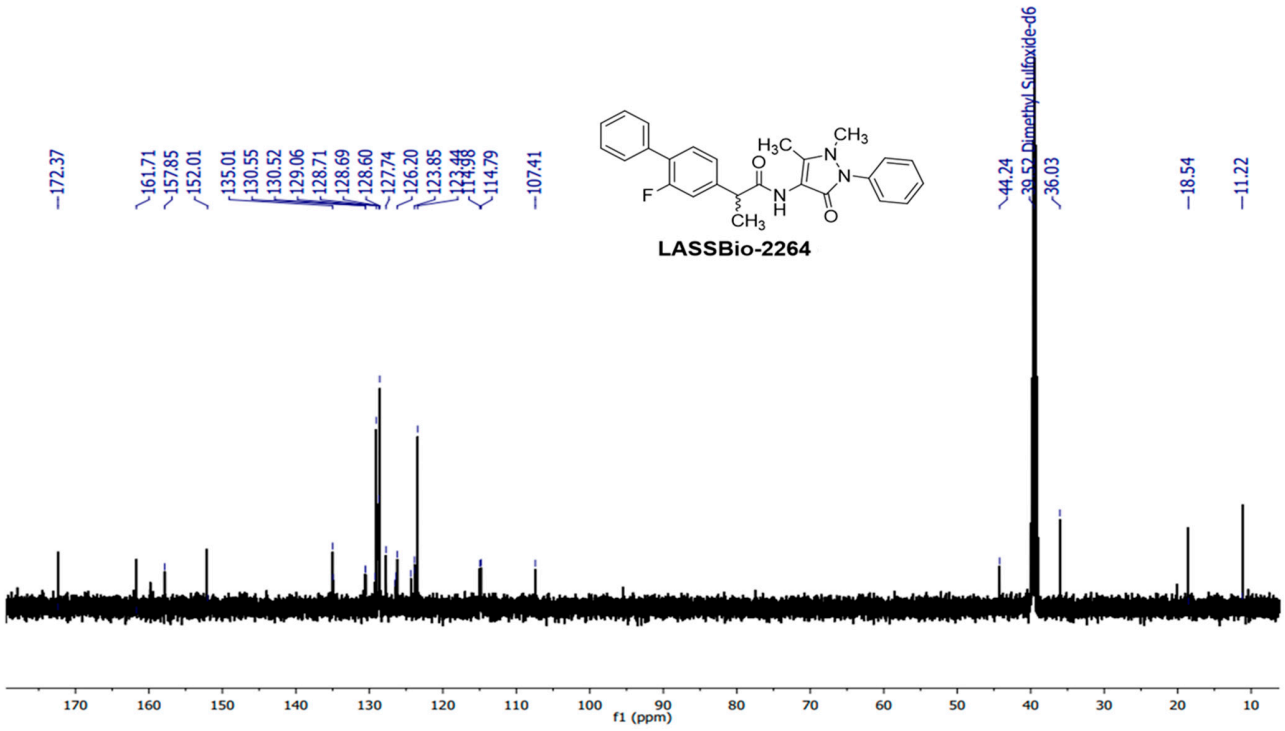

Figure S8. NMR spectrum ^{13}C pyrazolamide (**8**) (50 MHz, DMSO-d6).

<Chromatogram>

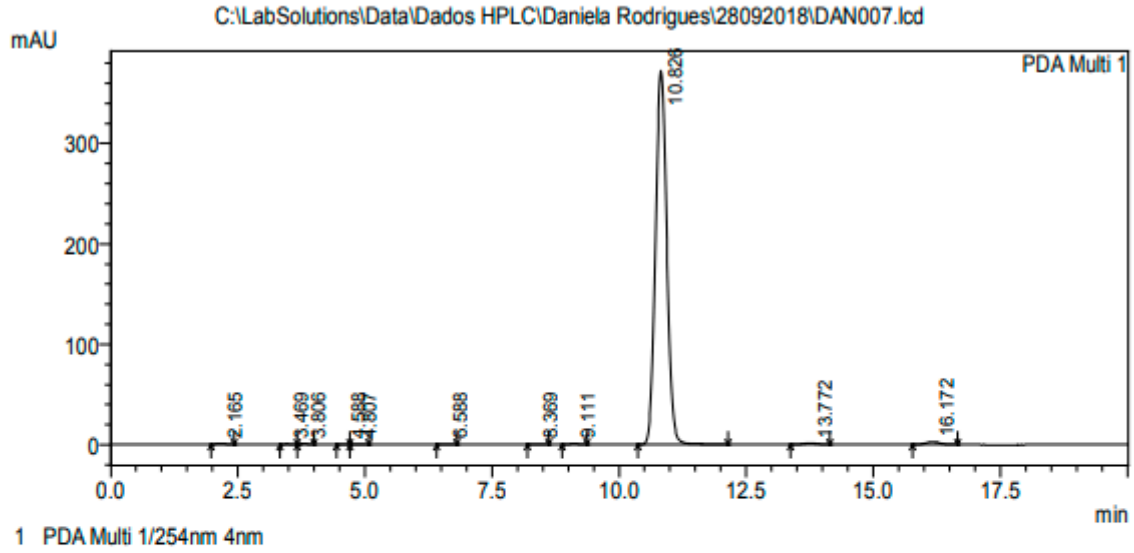

PeakTable

PDA Ch1 254nm 4nm

Peak#	Ret. Time	Area	Height	Area %	Height %
1	2.165	10192	740	0.174	0.195
2	3.469	3409	474	0.058	0.125
3	3.806	6968	964	0.119	0.254
4	4.588	1115	148	0.019	0.039
5	4.807	2137	222	0.036	0.059
6	6.588	3410	321	0.058	0.085
7	8.369	2188	179	0.037	0.047
8	9.111	9907	766	0.169	0.202
9	10.826	5757577	371270	98.024	97.920
10	13.772	24467	1332	0.417	0.351
11	16.172	52283	2740	0.890	0.723
Total		5873653	379155	100.000	100.000

Figure S9. Chromatogram obtained for **pyrazolamide** (8). Conditions: Shimadzu – LC20AD; Column: Kromasil 100-5 C18 250-4.6 mm; Mobile phase: 60% ACN, 40% water; Flow: 1mL/min; Detector: SPD-M20A (Diode Array); Wavelength: 254 nm.

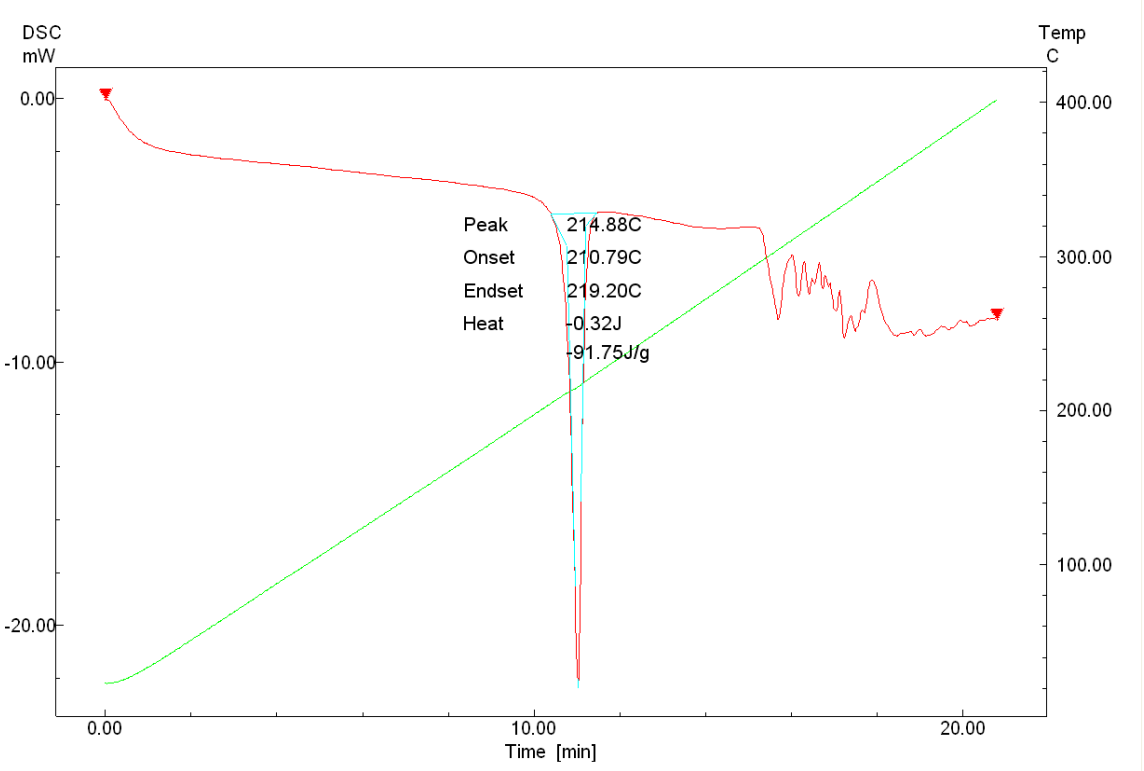

Figure S10. Determination of the melting point (FP) of pyrazolamide **(8)** determined by *Differential Scanning Calorimetry* (DSC) performed in a Shimadzu equipment (Model DSC-60).

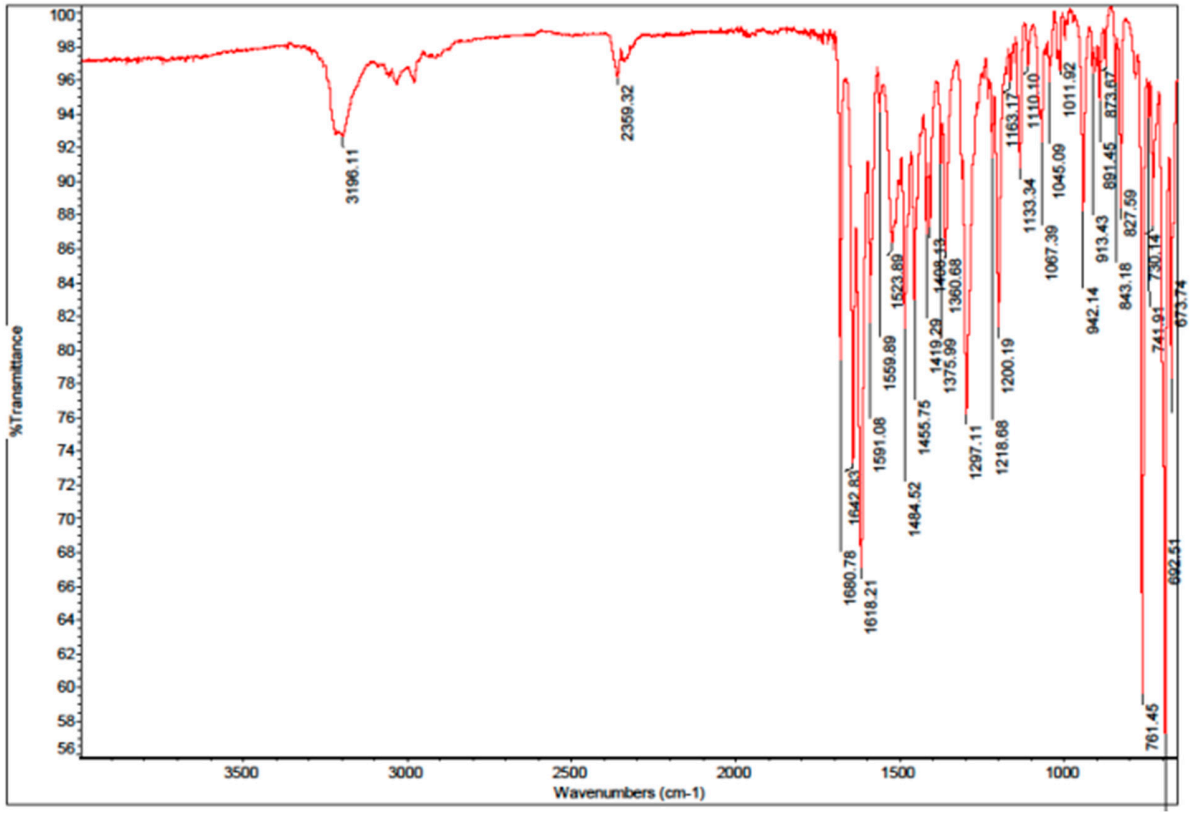

Figure S11. Infrared (ATR) of pyrazolamide (**8**).

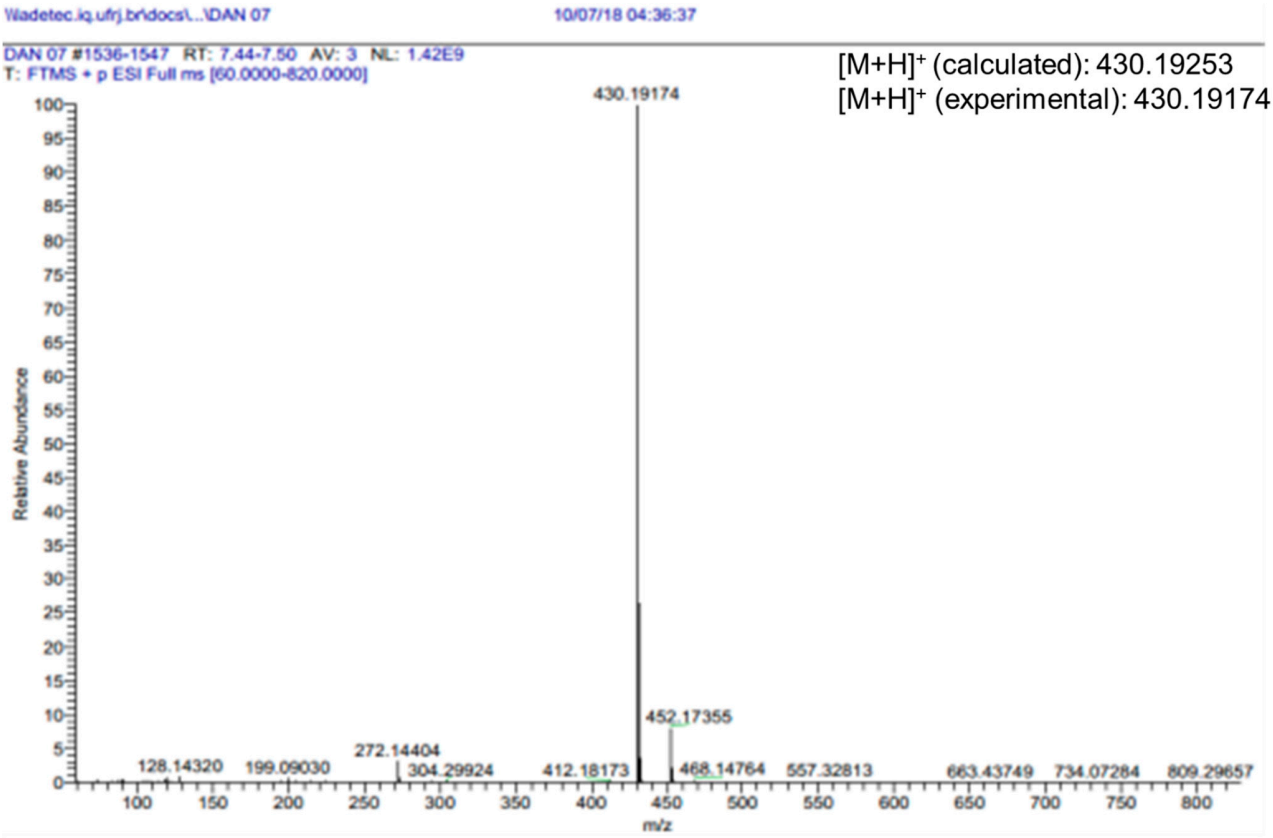

Figure S12. High resolution mass spectrum of pyrazolamide (**8**). Detection in positive mode ([M+H]⁺).

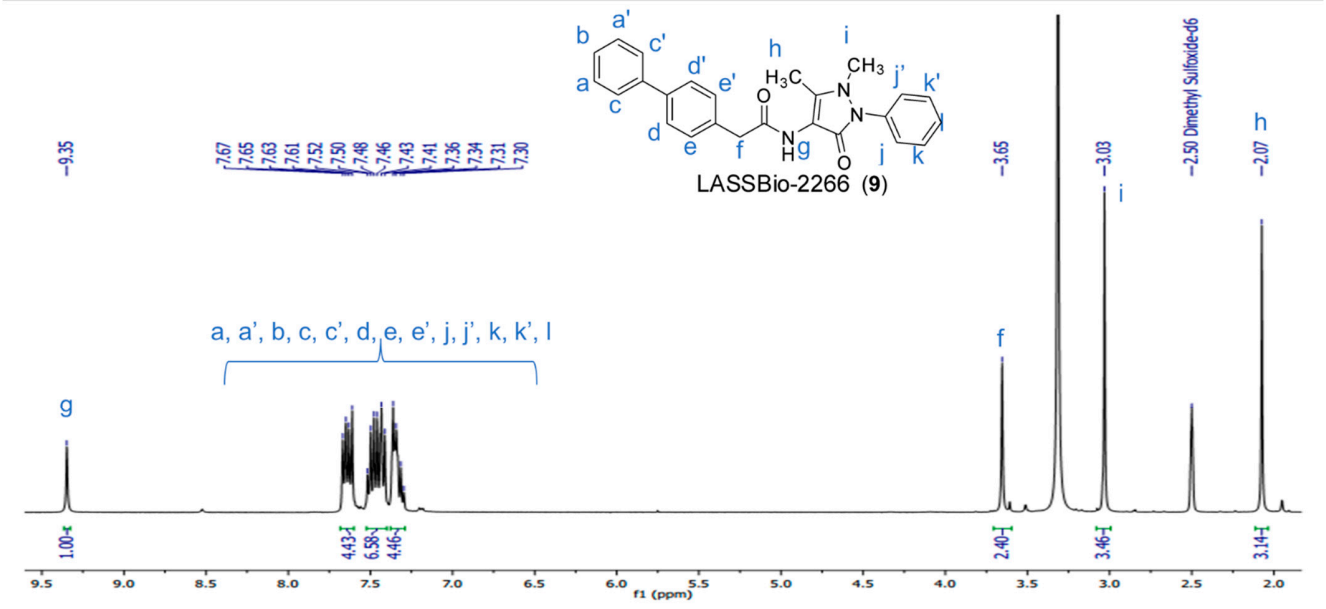

Figure S13. Spectrum¹H NMR pyrazolamide (**9**) (400 MHz, DMSO-d6).

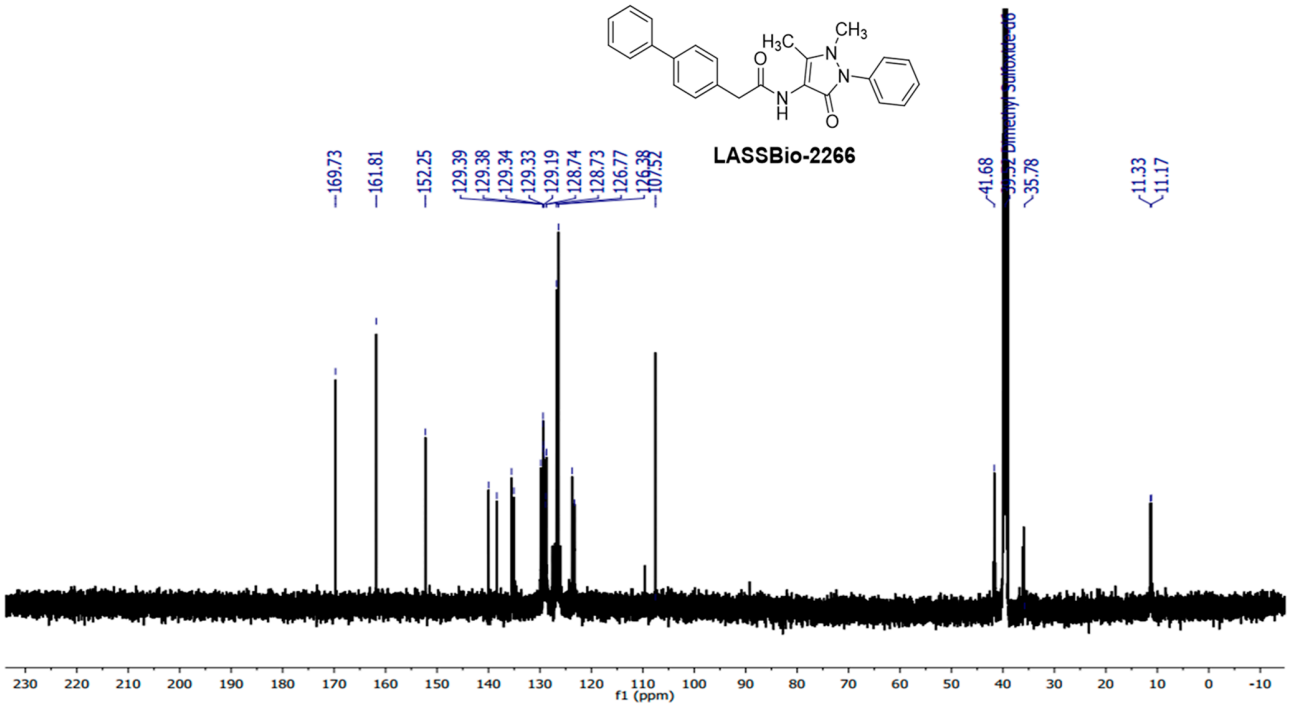

Figure S14. Spectrum ^{13}C NMR pyrazolamide **(9)** (50 MHz, DMSO-d6).

<Chromatogram>

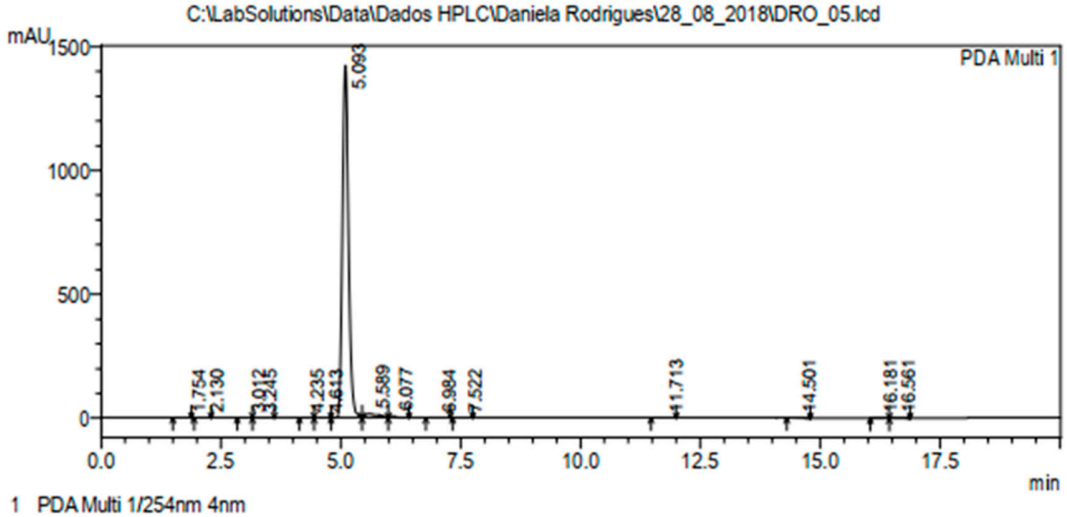

1 PDA Multi 1/254nm 4nm

PeakTable

PDA Ch1 254nm 4nm

Peak#	Ret. Time	Area	Height	Area %	Height %
1	1.754	2871	492	0.022	0.034
2	2.130	3414	299	0.027	0.021
3	3.012	4384	372	0.034	0.026
4	3.245	6721	765	0.052	0.053
5	4.235	1421	111	0.011	0.008
6	4.613	2185	212	0.017	0.015
7	5.093	12443500	1423276	96.605	98.228
8	5.589	335900	15853	2.608	1.094
9	6.077	50987	5034	0.396	0.347
10	6.984	14408	1414	0.112	0.098
11	7.522	3283	312	0.025	0.022
12	11.713	4971	373	0.039	0.026
13	14.501	2567	176	0.020	0.012
14	16.181	1723	95	0.013	0.007
15	16.561	2521	166	0.020	0.011
Total		12880854	1448949	100.000	100.000

Figure S15. Chromatogram obtained for pyrazolamide (**9**). Conditions: Shimadzu – LC20AD; Column: Kromasil 100-5 C18 250-4.6 mm; Mobile phase: 60% ACN, 40% water; Flow: 1mL/min; Detector: SPD-M20A (Diode Array); Wavelength: 254 nm.

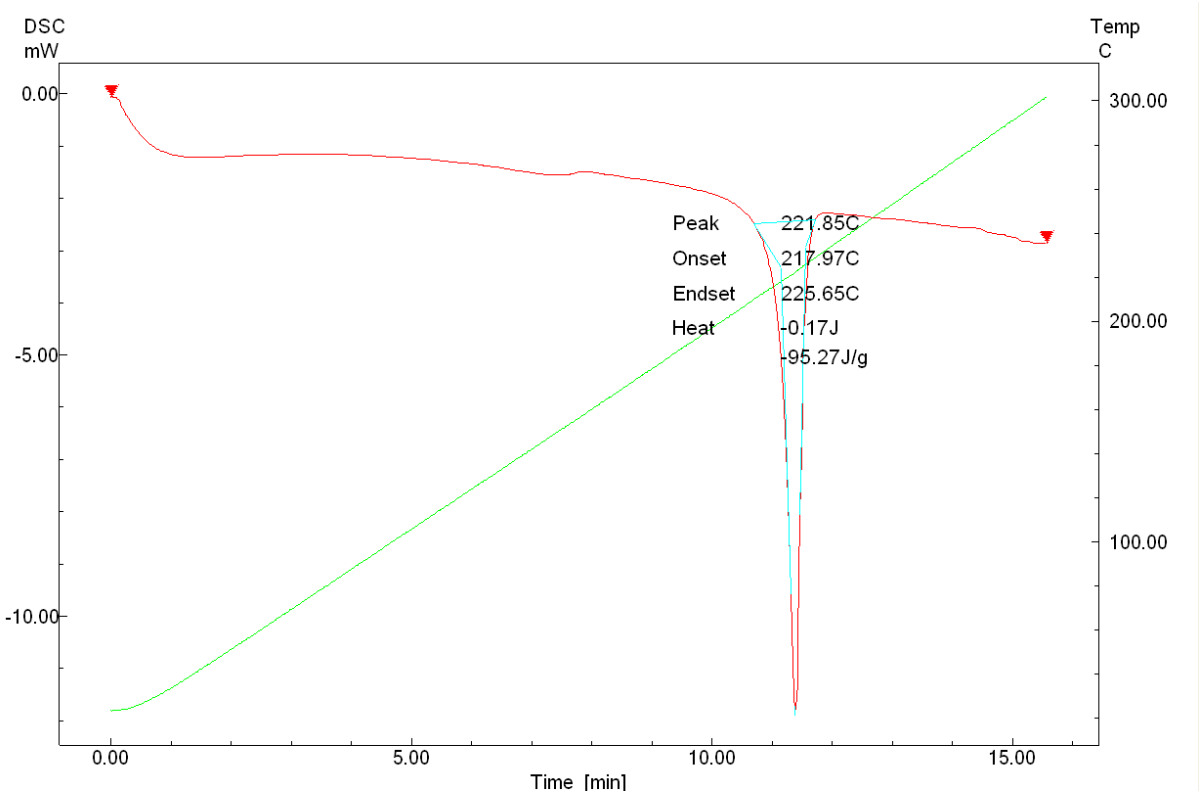

Figure S16. Determination of the melting point (FP) of pyrazolamide **(9)** determined by *Differential Scanning Calorimetry* (DSC) performed in a Shimadzu equipment (Model DSC-60).

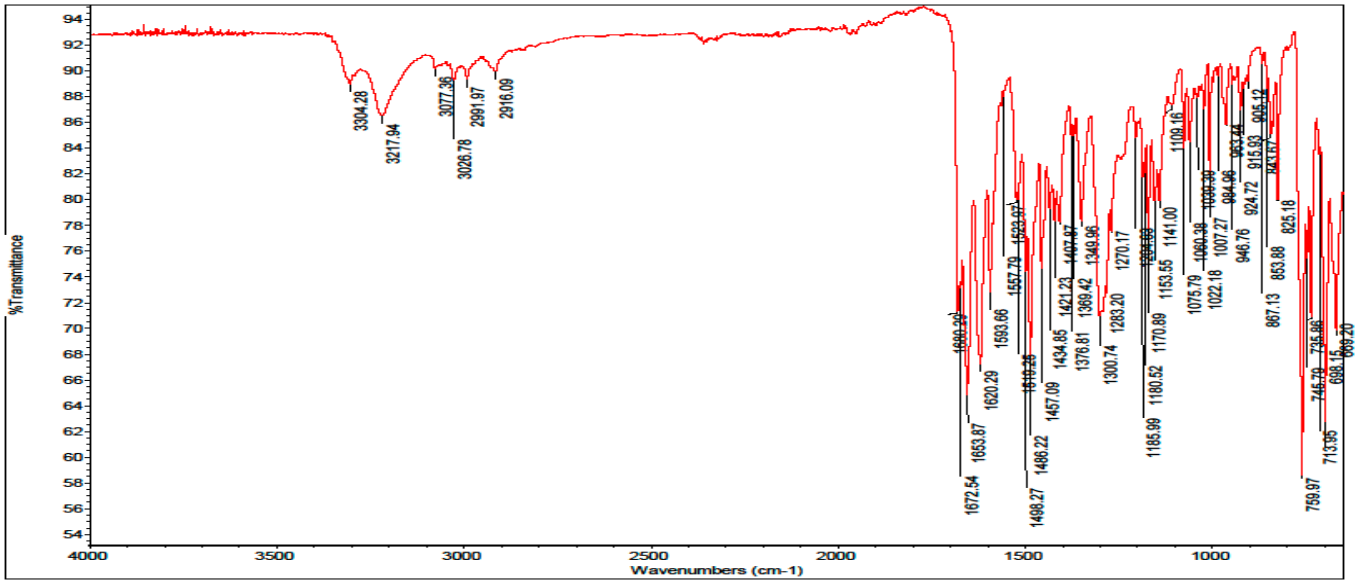

Figure S17. Infrared (ATR) pyrazolamide **(9)**.

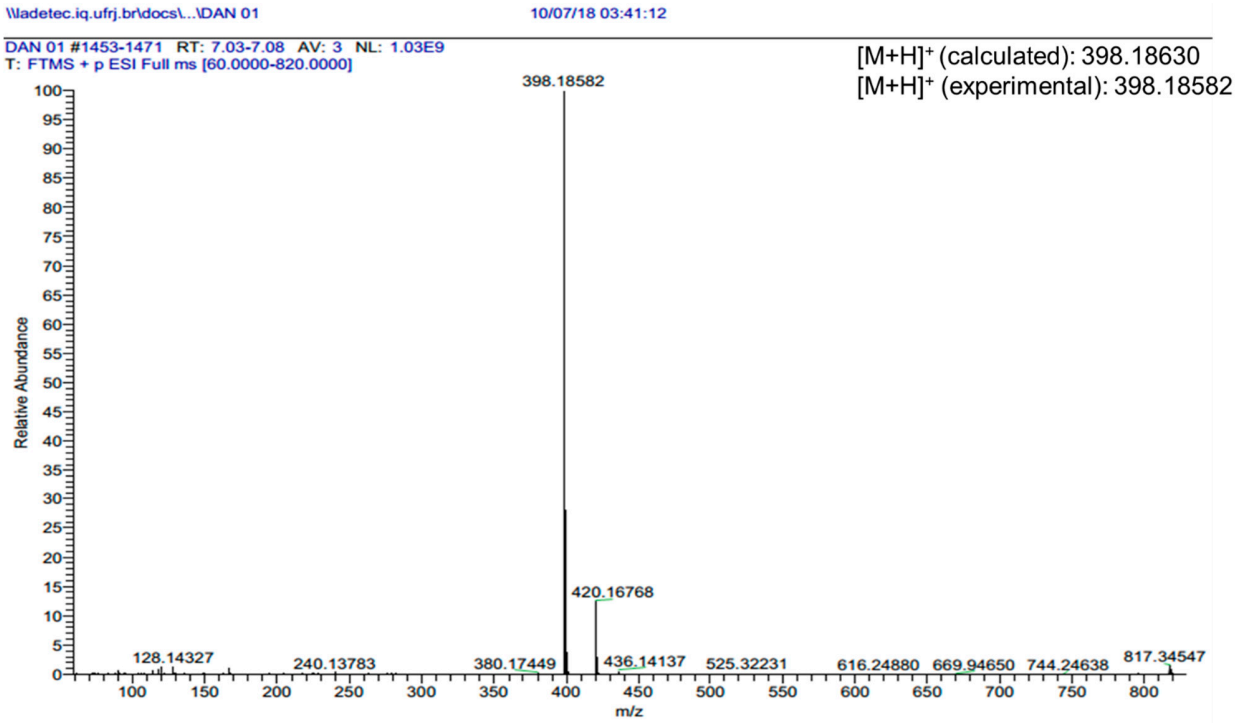

Figure S18. High resolution mass spectrum of pyrazolamide **(9)**. Detection in positive mode ($[M+H]^+$).

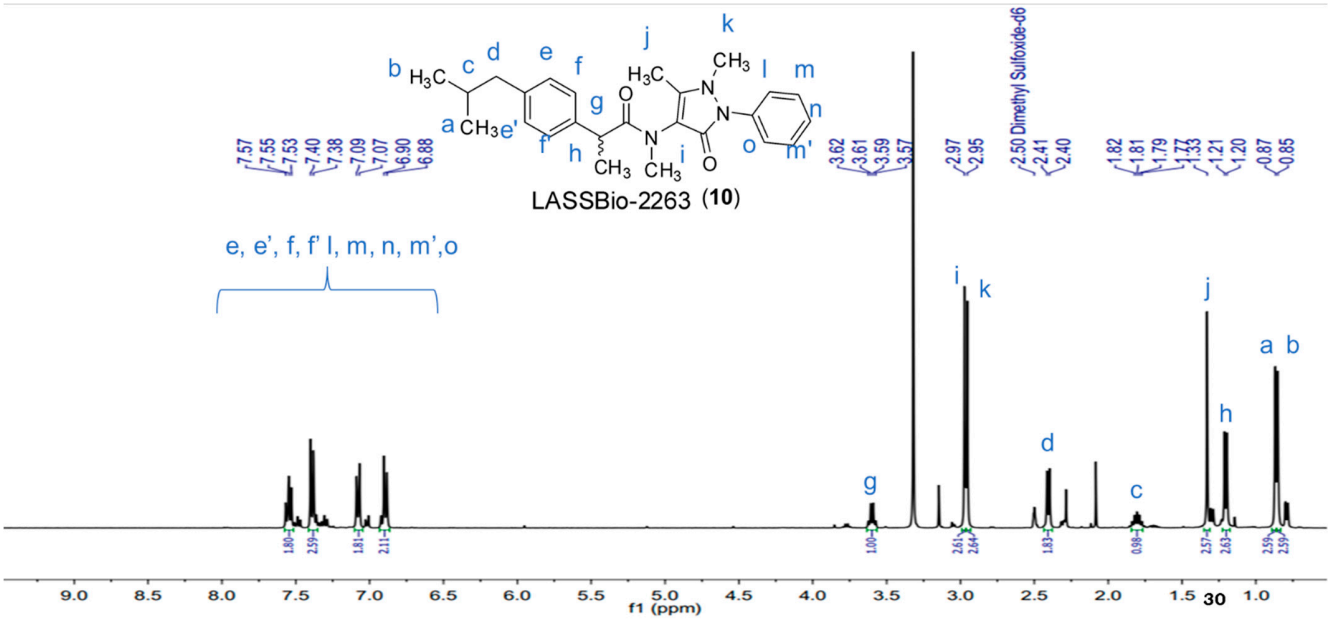

Figure S19. [1]H NMR spectrum of pyrazolamide (**10**) (400 MHz, DMSO-d6).

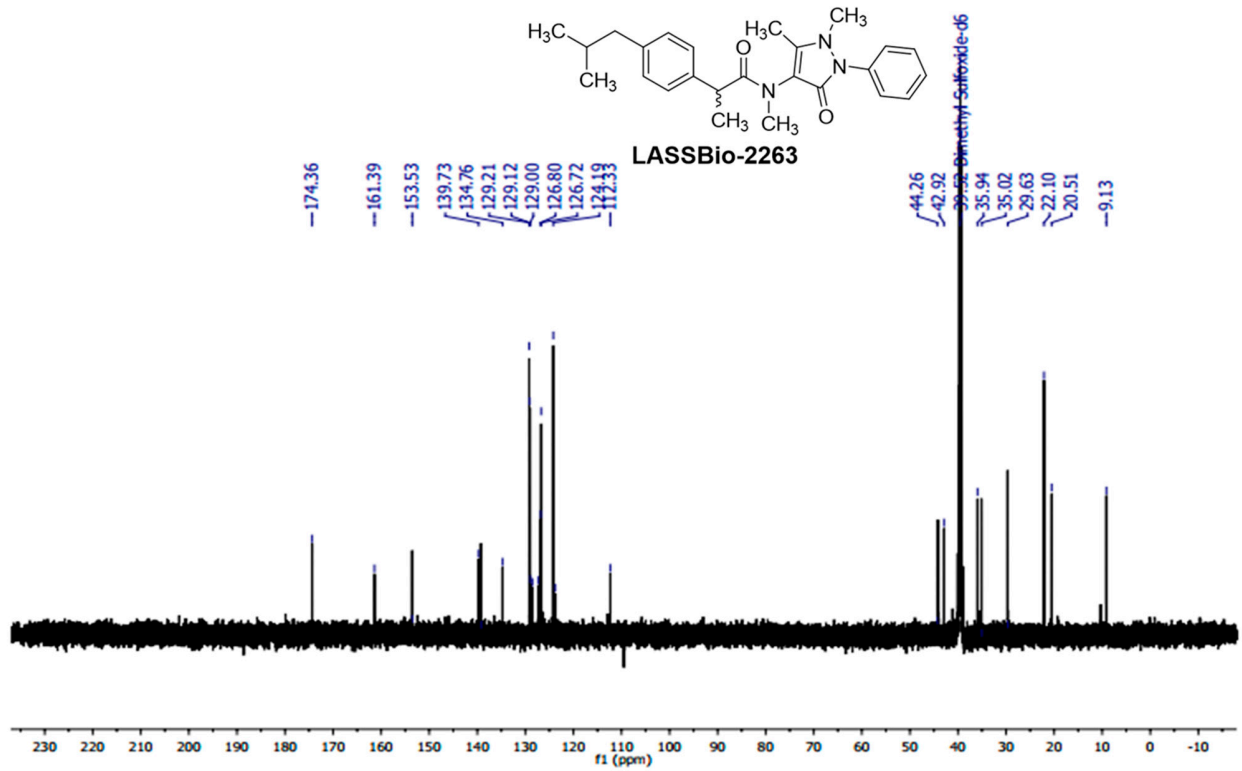

Figure S20. NMR spectrum [13]C of pyrazolamide (**10**) (50 MHz, DMSO-d6).

<Chromatogram>

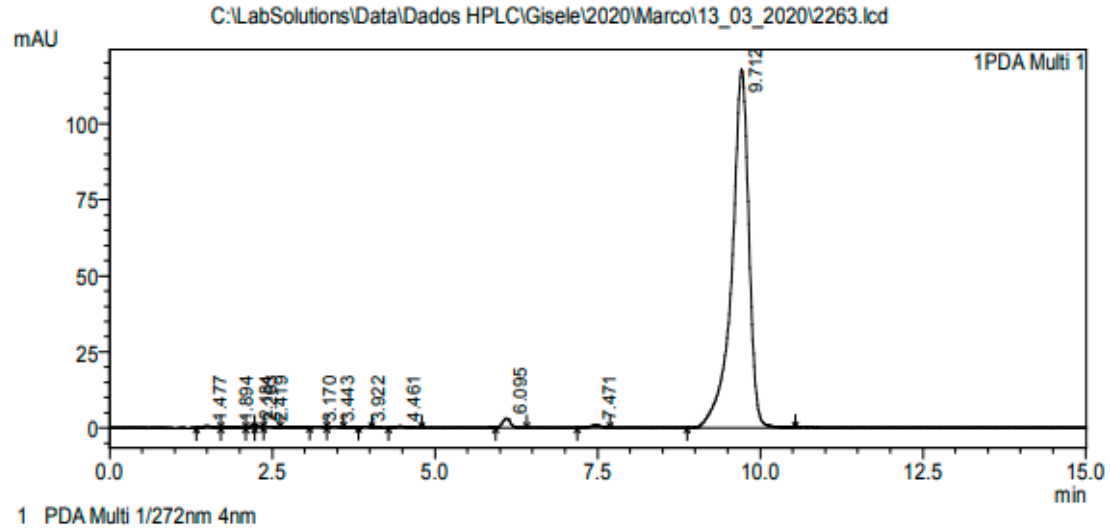

PeakTable

PDA Ch1 272nm 4nm

Peak#	Ret. Time	Area	Height	Area %	Height %
1	1.477	5457	600	0.248	0.479
2	1.894	2871	293	0.130	0.234
3	2.184	2958	901	0.134	0.719
4	2.263	3140	583	0.143	0.465
5	2.419	1917	221	0.087	0.177
6	3.170	2023	202	0.092	0.161
7	3.443	1637	239	0.074	0.191
8	3.922	2200	350	0.100	0.279
9	4.461	4727	416	0.215	0.332
10	6.095	26490	3082	1.204	2.460
11	7.471	9913	815	0.451	0.650
12	9.712	2136763	117604	97.121	93.854
Total		2200096	125305	100.000	100.000

Figure S21. Chromatogram obtained for pyrazolamide (**10**). Conditions: Shimadzu – LC20AD; Column: Kromasil 100-5 C18 250-4.6 mm; Mobile phase: 60% ACN, 40% water; Flow: 1mL/min; Detector: SPD-M20A (Diode Array); Wavelength: 272 nm.

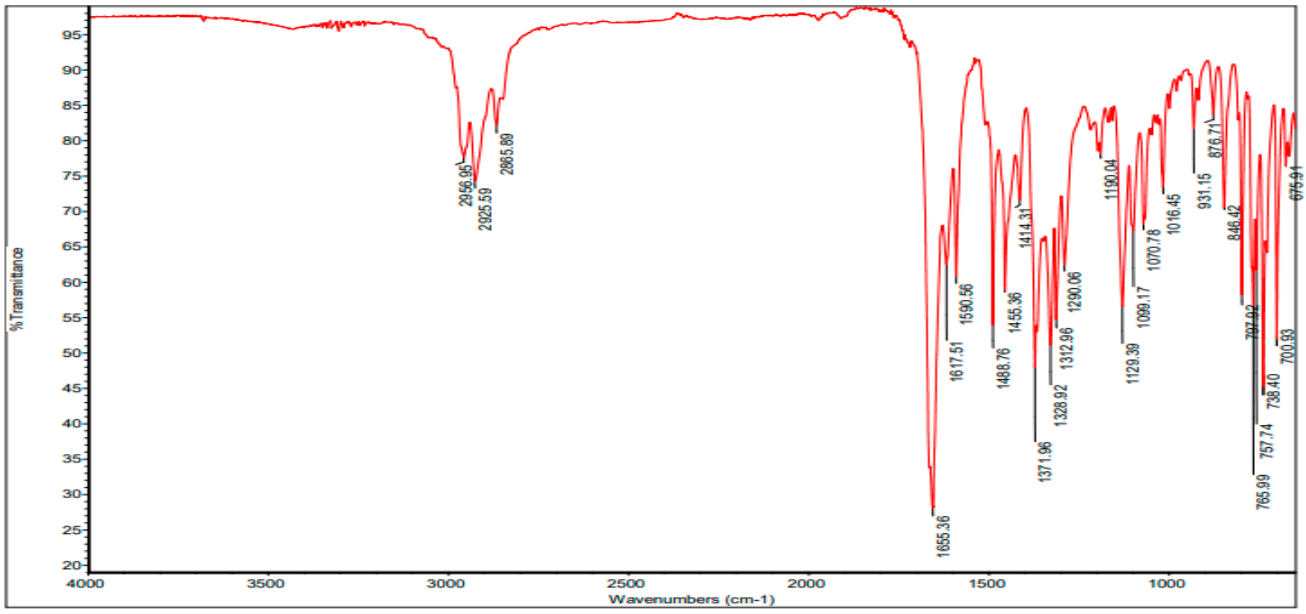

Figure S22. Infrared (ATR) pyrazolamide **(10)**.

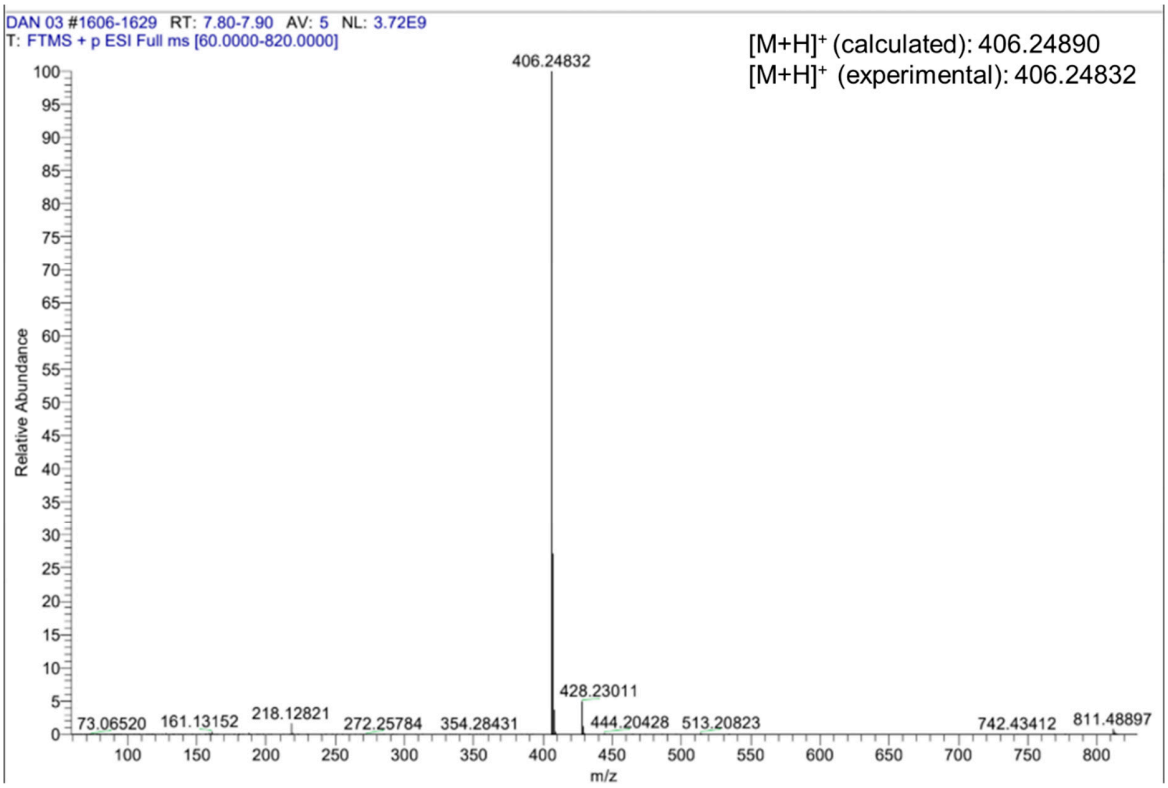

Figure S23. High resolution mass spectrum of pyrazolamide **(10)**. Detection in positive mode ($[M+H]^+$).

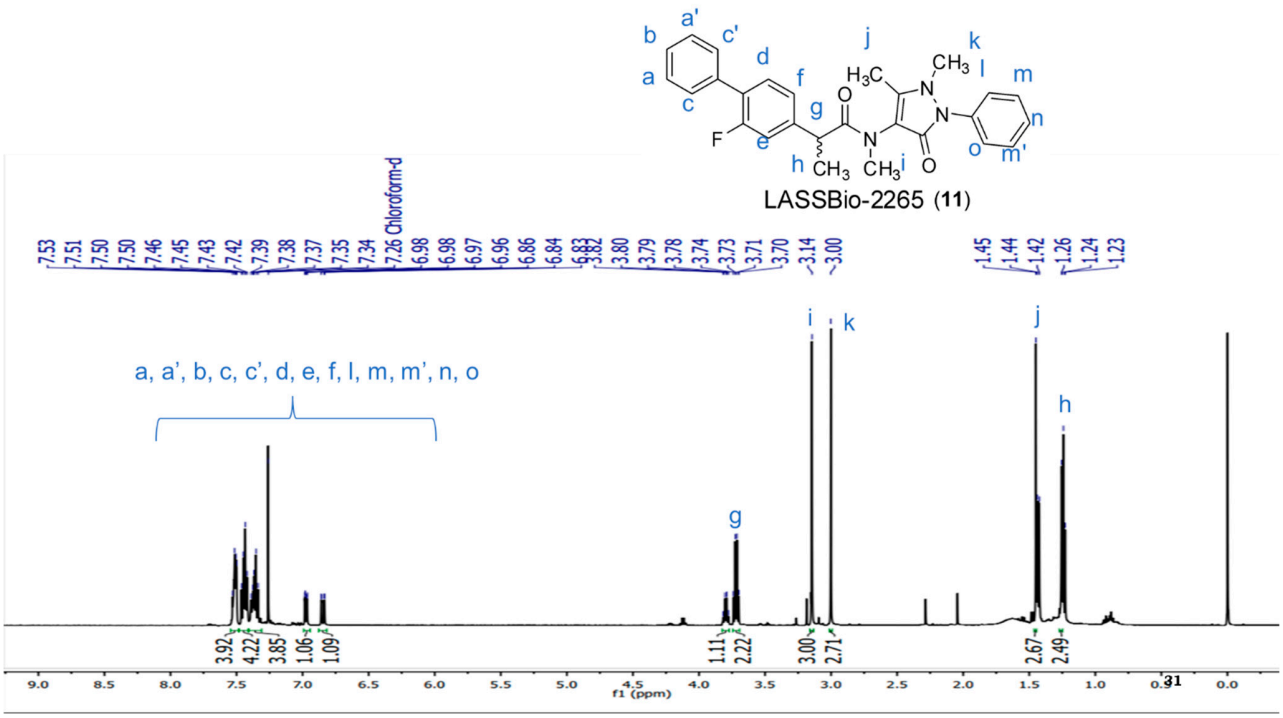

Figure S24. Spectrum of RMN[1]H to **LASSBio-2265 (11)** (500 MHz, acetonitrile-*d*3).

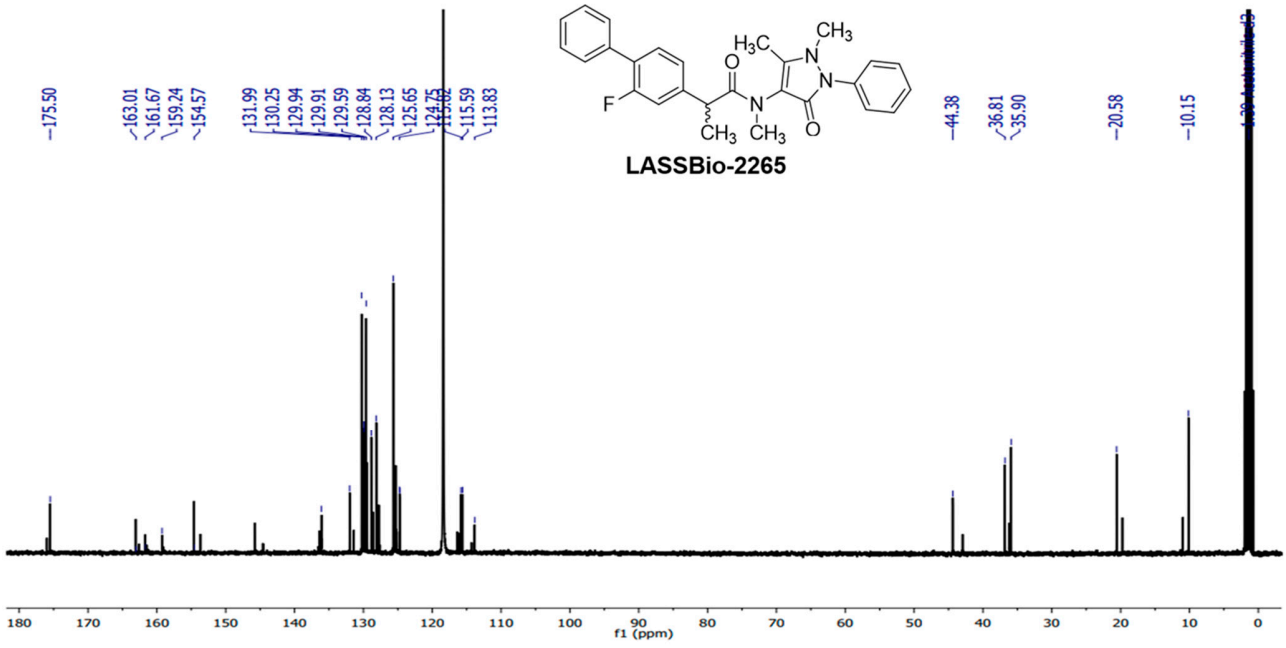

Figure S25. NMR spectrum [13]C of **LASSBio-2265** (**11**) (100 MHz, $CDCl_3$).

<Chromatogram>

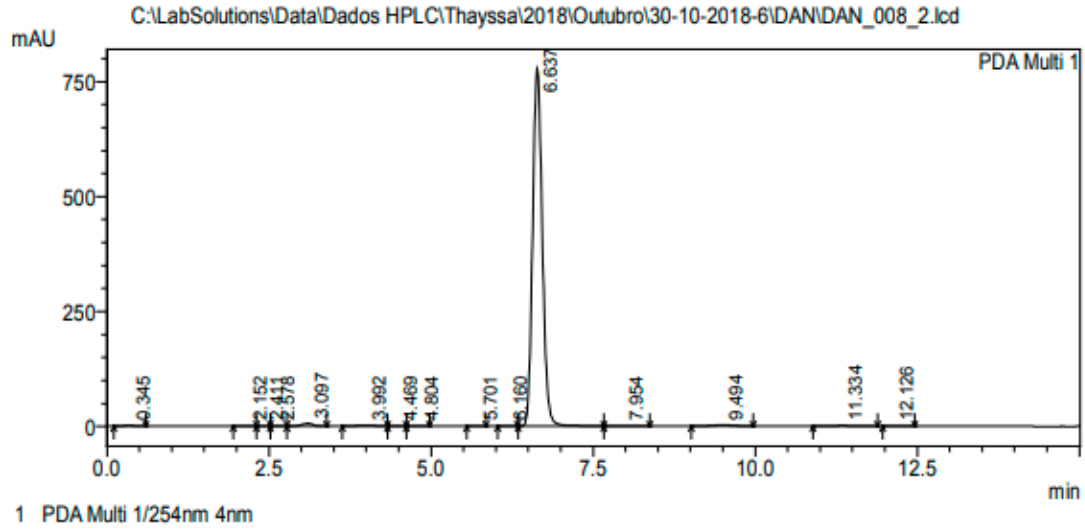

PeakTable

PDA Ch1 254nm 4nm

Peak#	Ret. Time	Area	Height	Area %	Height %
1	0.345	16092	1310	0.194	0.165
2	2.152	8175	613	0.098	0.077
3	2.411	2178	220	0.026	0.028
4	2.578	2817	355	0.034	0.045
5	3.097	70327	5795	0.846	0.732
6	3.992	32786	1689	0.394	0.213
7	4.469	1933	131	0.023	0.017
8	4.804	2867	344	0.034	0.043
9	5.701	1696	201	0.020	0.025
10	6.160	1027	105	0.012	0.013
11	6.637	8083227	776741	97.248	98.123
12	7.954	11066	542	0.133	0.069
13	9.494	55177	2446	0.664	0.309
14	11.334	19397	888	0.233	0.112
15	12.126	3201	224	0.039	0.028
Total		8311964	791603	100.000	100.000

Figure S26. Chromatogram obtained for **LASSBio-2265** (**11**). Conditions: Shimadzu – LC20AD; Column: Kromasil 100-5 C18 250-4.6 mm; Mobile phase: 60% ACN, 40% water; Flow: 1mL/min; Detector: SPD-M20A (Diode Array); Wavelength: 254 nm.

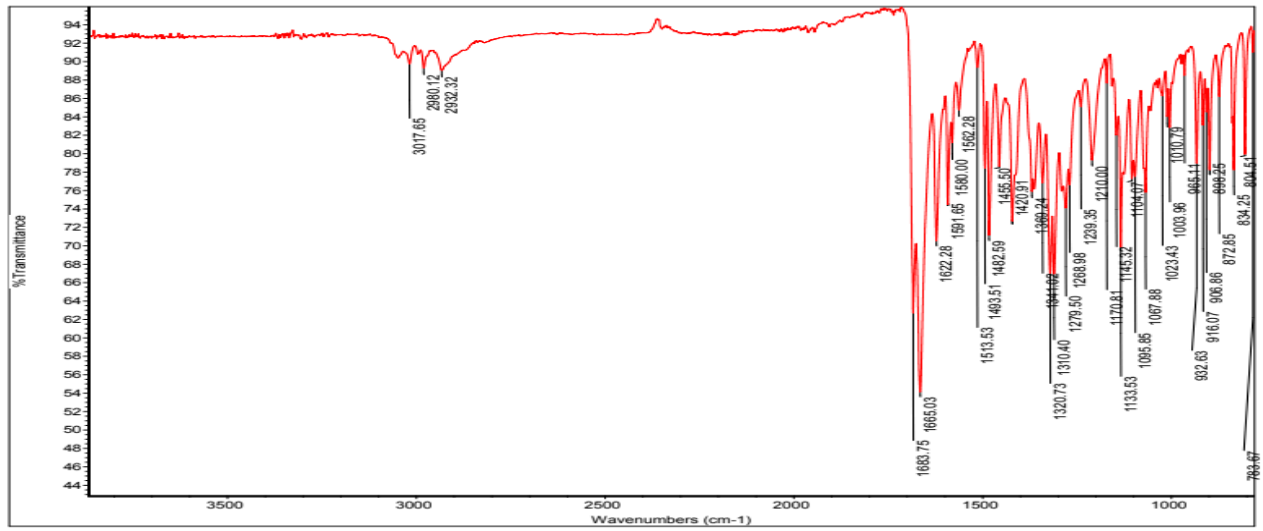

Figure S27. Infrared (ATR) of **LASBio-2265** (**11**).

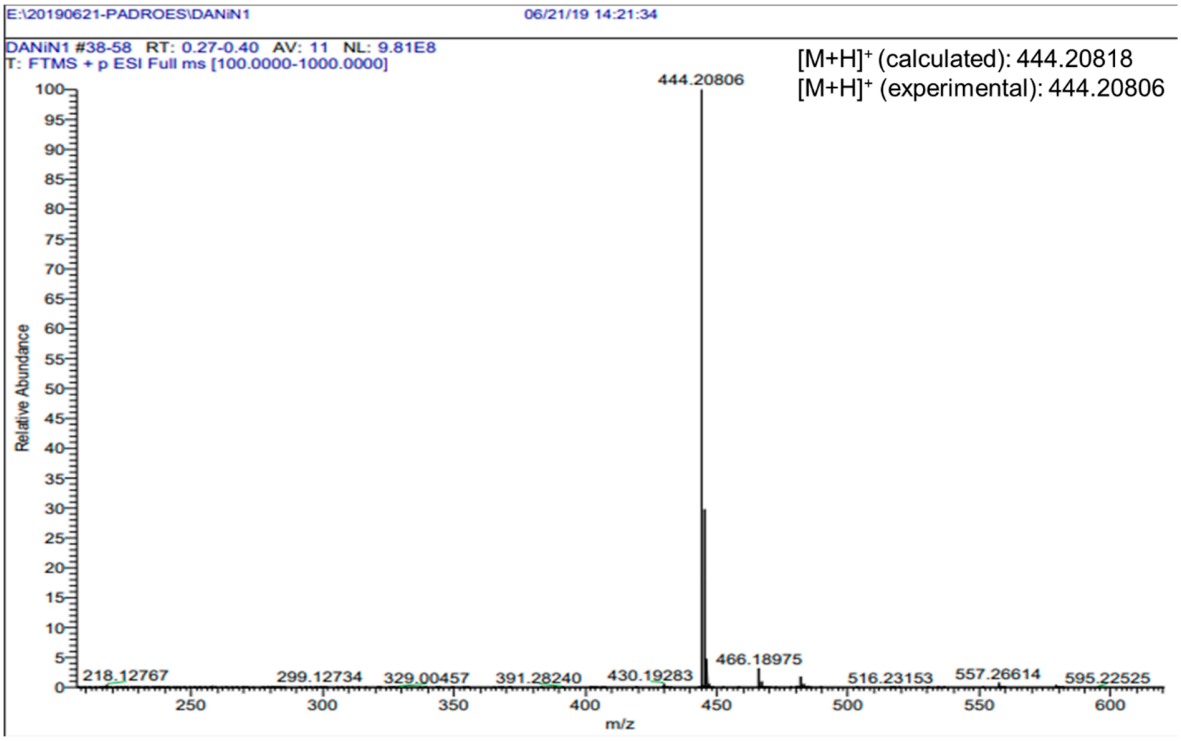

Figure S28. High resolution mass spectrum of **LASSBio-2265** (**11**). Detection in positive mode ([M+H]$^+$).

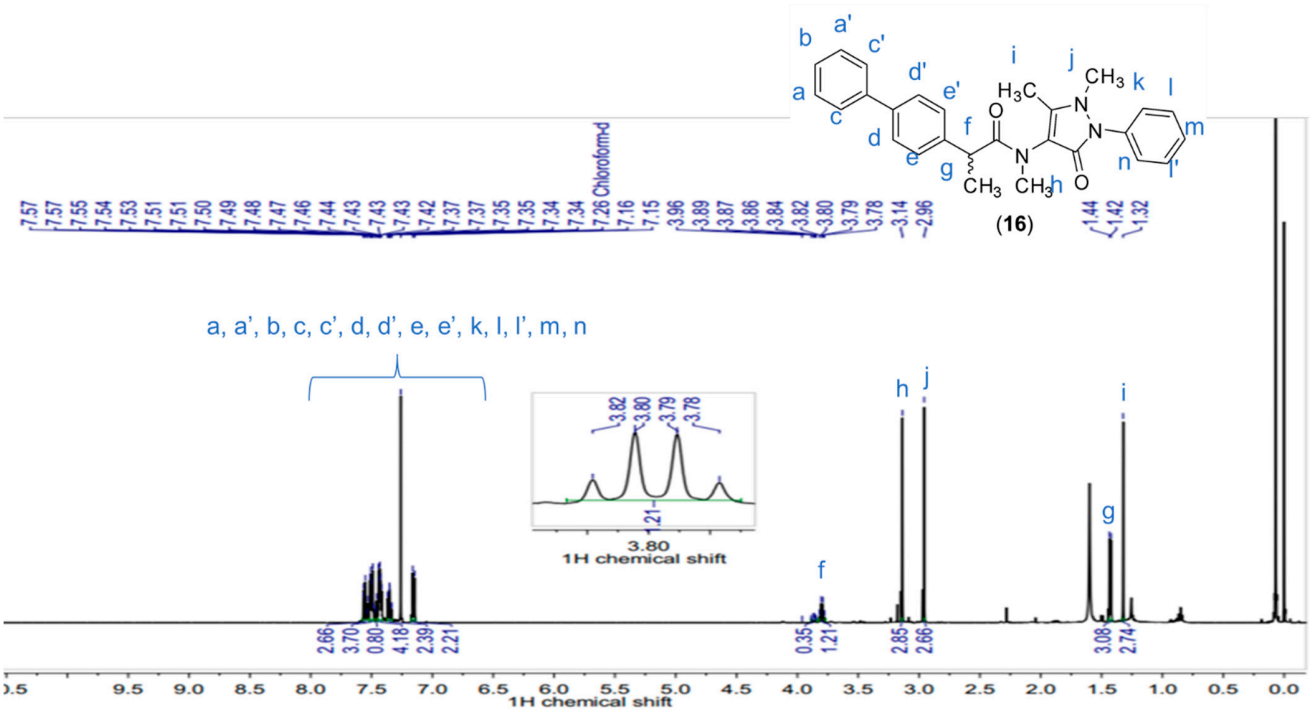

Figure S29. [1]H NMR spectrum[1]of bismethylated pyrazolamide **(16)** (400 MHz, $CDCl_3$).

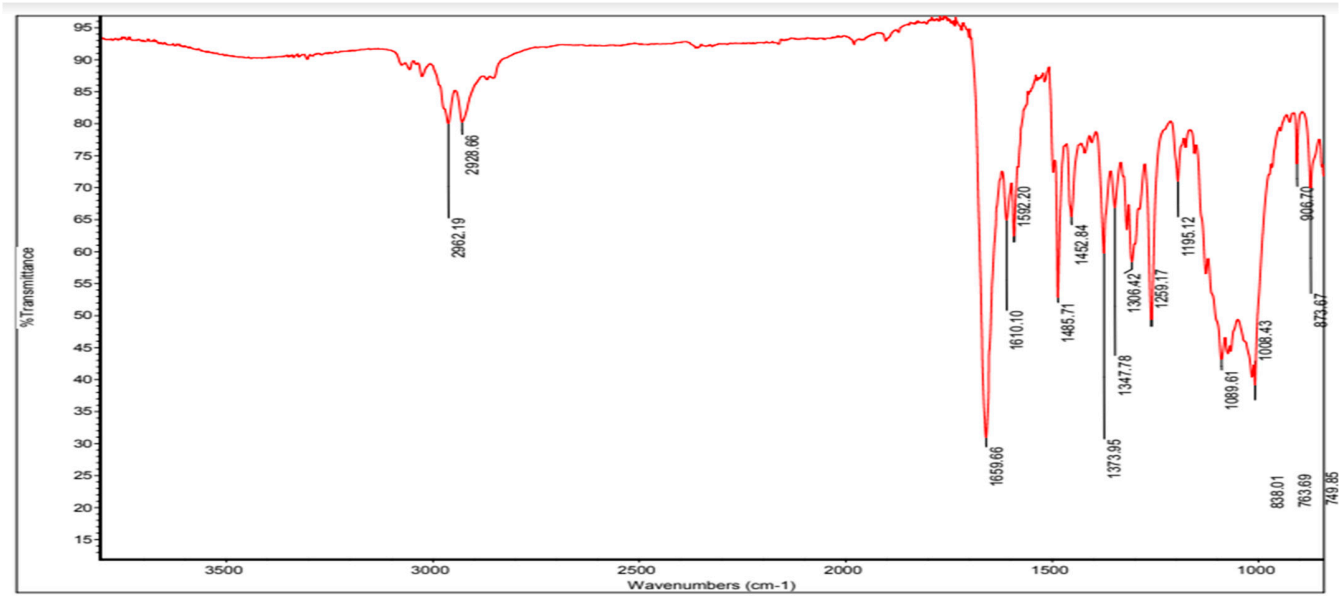

Figure S30. Infrared (ATR) of bismethylated pyrazolamide **(16)**.

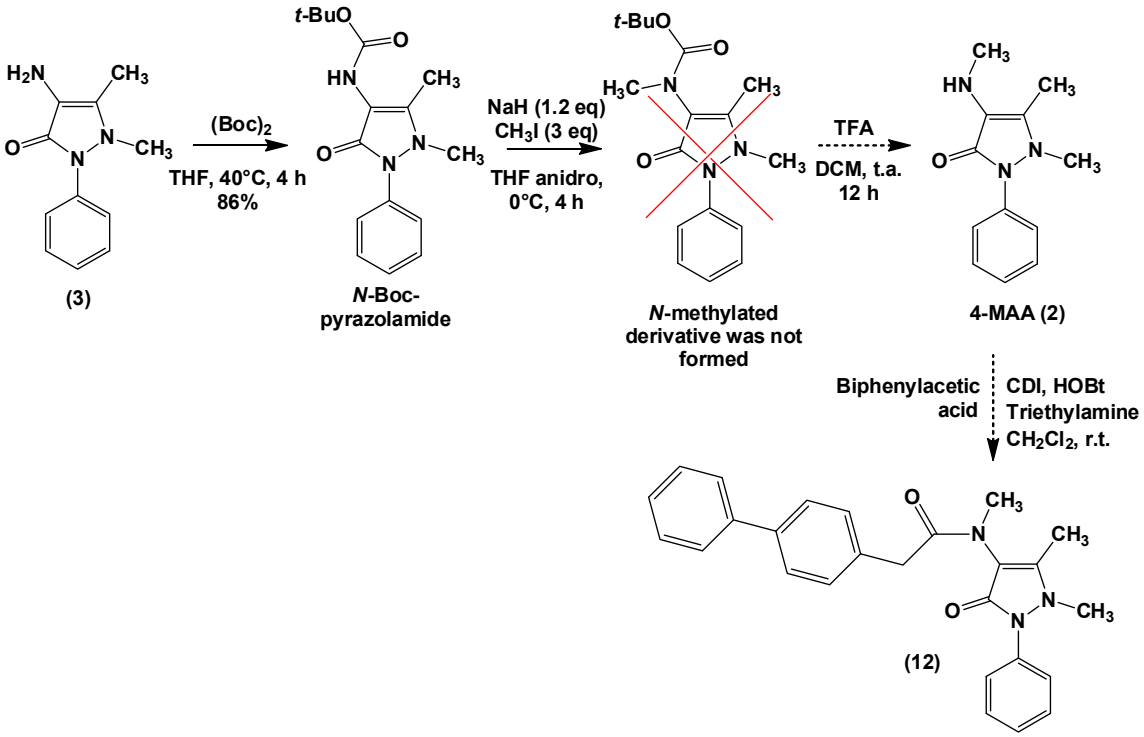

Figure S31. Alternative methodology tried for the synthesis of pyrazolamide (**12**).

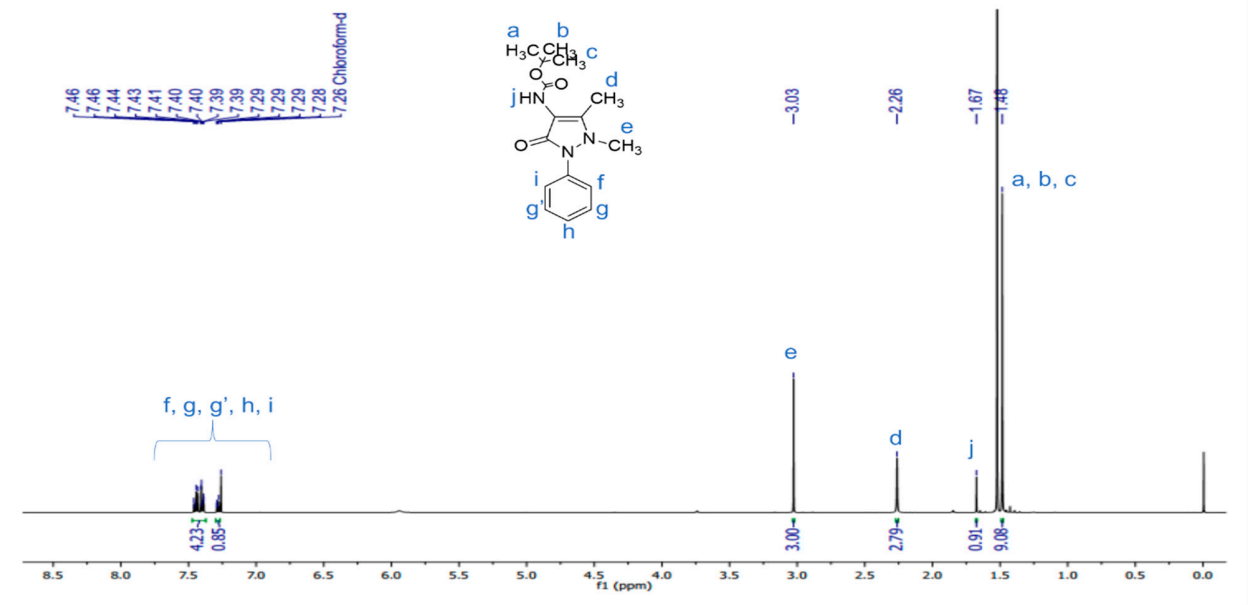

Figura S32. ^{1}H NMR spectrum[1]of N-Boc-pyrazolamide (500 MHz, $CDCl_3$).

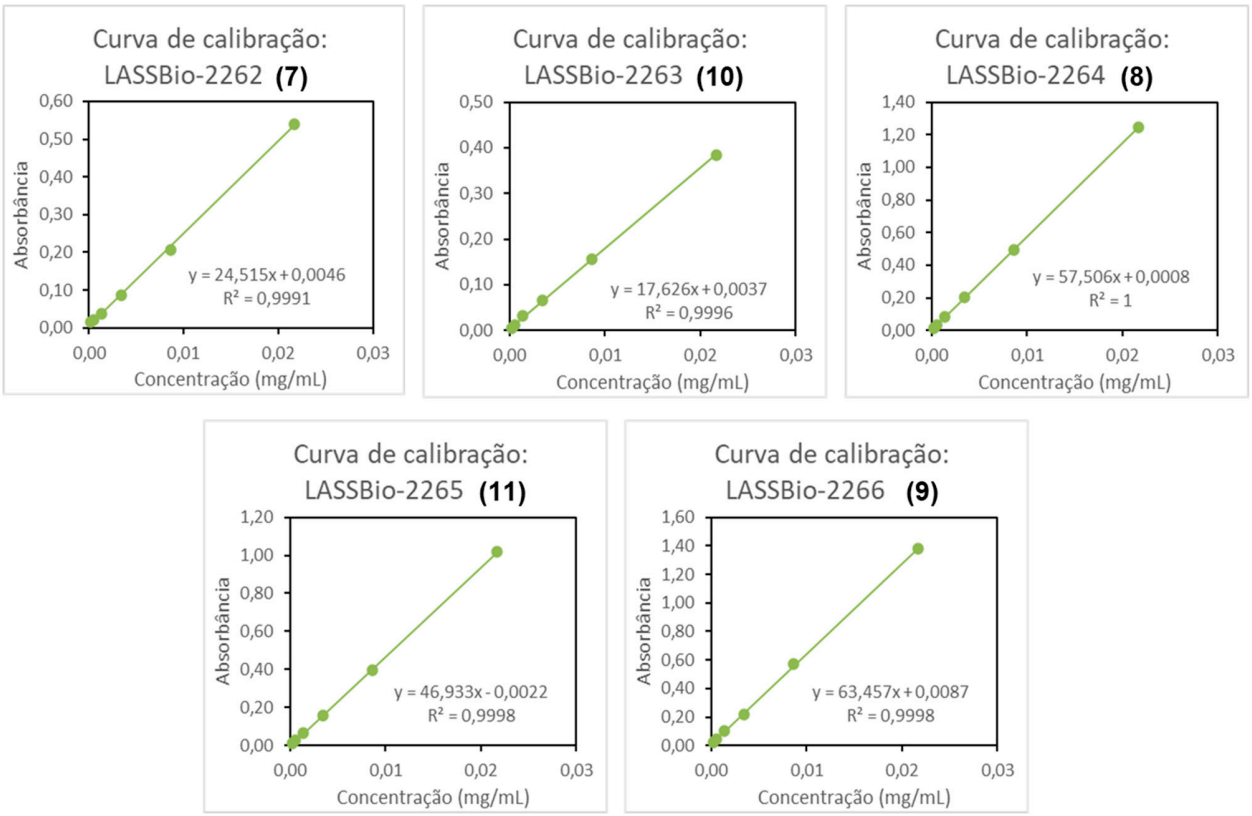

Figure S33. Calibration curves for determination of aqueous solubility of the pyrazolamides (**7-11**).

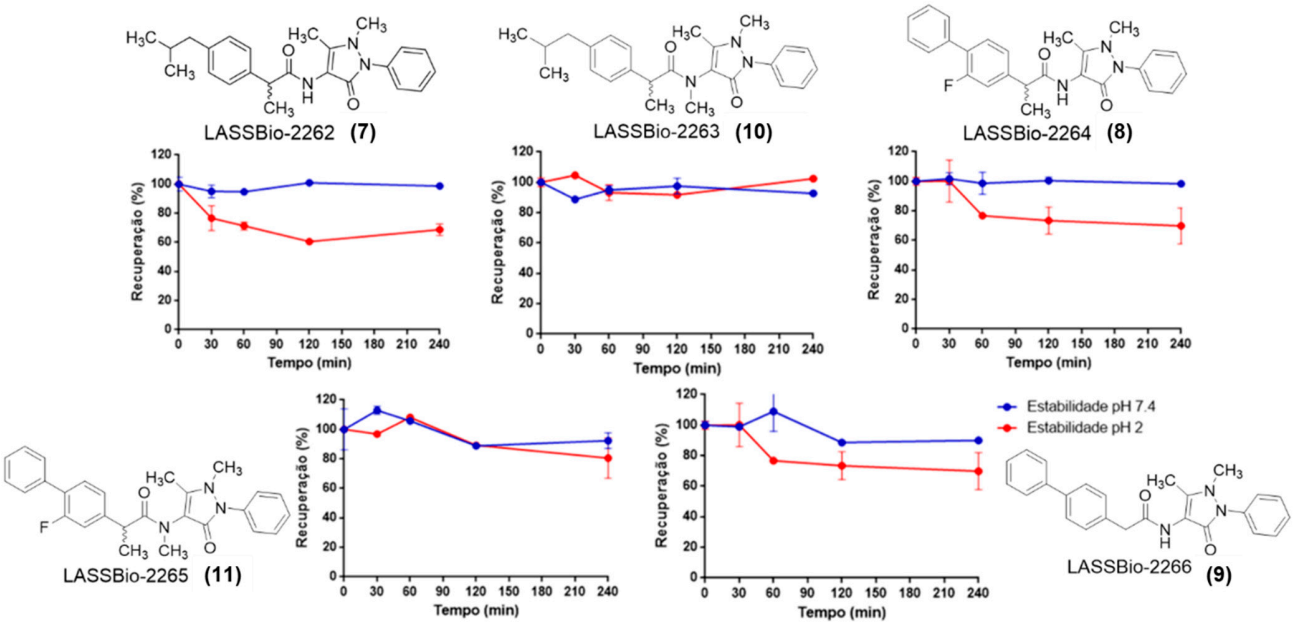

Figure S34. Chemical stability of pyrazolamides (**7-11**) at pH 2 (red) and pH 7.4 (blue). Experiments performed in triplicate. Reading performed in HPLC-PDA (Shimadzu-LC20A; Kromasil C-18 column (4.6mm x 250mm); SPD-M20A detector (Diode Array); flow: 1ml/minute]; Mobile phase: Acetonitrile:water, 40%. Wavelength: 272 nm (**LASSBio-2262** (**7**) and **LASSBio-2263** (**10**)), 247 nm (**LASSBio-2264** (**8**) and **LASSBio-2265** (**11**)) and 253 nm (**LASSBio-2266** (**9**)) The calculations were performed according to the peak area values of the analytes.

Table S1. Absorbed fraction of drugs used as standard and pyrazolamides **(7-11)** determined in the PAMPA-GTI model.

COMPOUND	Pe** Lit (10^{-6}cm/s)	Pe** Exp (10^{-6} cm/s)	Fa# (%)	Classification
Acyclovir*	0,06	0,08	2,98	LOW
Atenolol*	0,1	0,11	4,22	LOW
Ranitidine*	0,5	0,38	13,48	LOW
Sulfassalazine*	0,3	0,45	15,5	LOW
Aspirin*	3,8	1,69	47,36	AVERAGE
Hydrocortisone*	3,4	2,16	55,93	AVERAGE
Prednisone*	5,7	3,09	69,16	AVERAGE
Ketoconazole*	3,3	4,93	84,68	HIGH
Coumarin*	22,9	22,65	99,98	HIGH
Diclofenac*	12,5	13,01	99,28	HIGH
Verapamil*	7,4	6,45	91,40	HIGH
(7)	**-**	**15,38**	**99,71**	**HIGH**
(10)	**-**	**9,15**	**96,91**	**HIGH**
(8)	**-**	**9,69**	**97,49**	**HIGH**
(11)	**-**	**10,18**	**97,91**	**HIGH**
(9)	**-**	**11,00**	**98,47**	**HIGH**

*Drugs used as standard for experimental validation. **Pe= permeability coefficient; #Fa= absorbed fraction (ZHU et al., 2002).

Table S2. Permeability of drugs used as standard, and pyrazolamides **(7-11)** determined in the PAMPA-BBB model.

Compound	**Pe literatura (10-6 cm s-1)**	**Pe experimental (10-6 cm s-1)**	**Classification**
Atenolol	**0,8**	**0,46**	**CNS -**
Caffeine	**1,3**	**0,81**	**CNS -**
Diazepam	**16**	**14,30**	**CNS +**
Enoxacin	**0,9**	**0,53**	**CNS -**
Ofloxacin	**0,8**	**1,29**	**CNS -**
Testosterone	**17**	**16,85**	**CNS +**
Verapamil	**16**	**15,40**	**CNS +**
(7)	**-**	**12,77**	**CNS +**
(10)	**-**	**12,68**	**CNS +**
(8)	**-**	**17,25**	**CNS +**
(11)	**-**	**9,26**	**CNS +**
(9)	**-**	**4,51**	**CNS +**

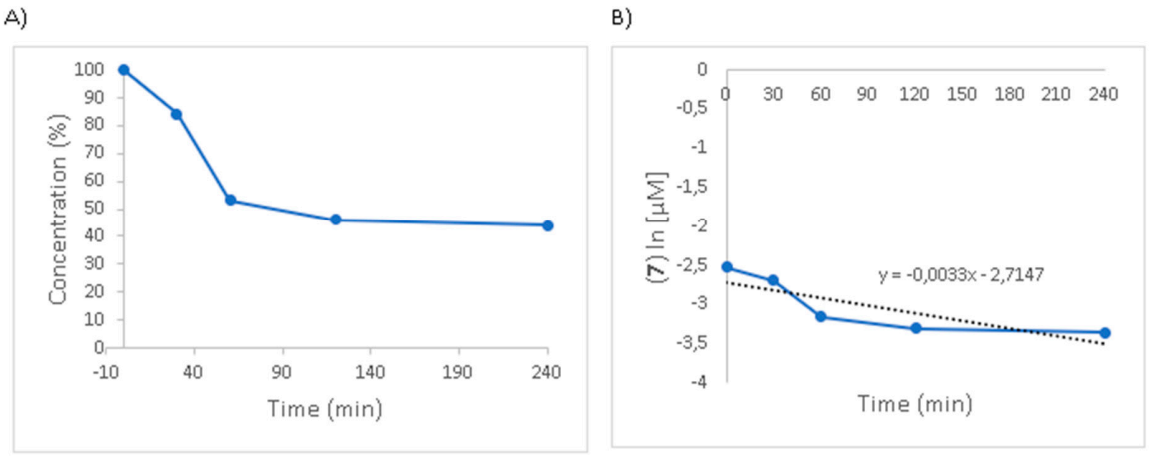

Figure S35. A) Plasma stability profile of (**7**); B) First order rate constant (k) for elimination.

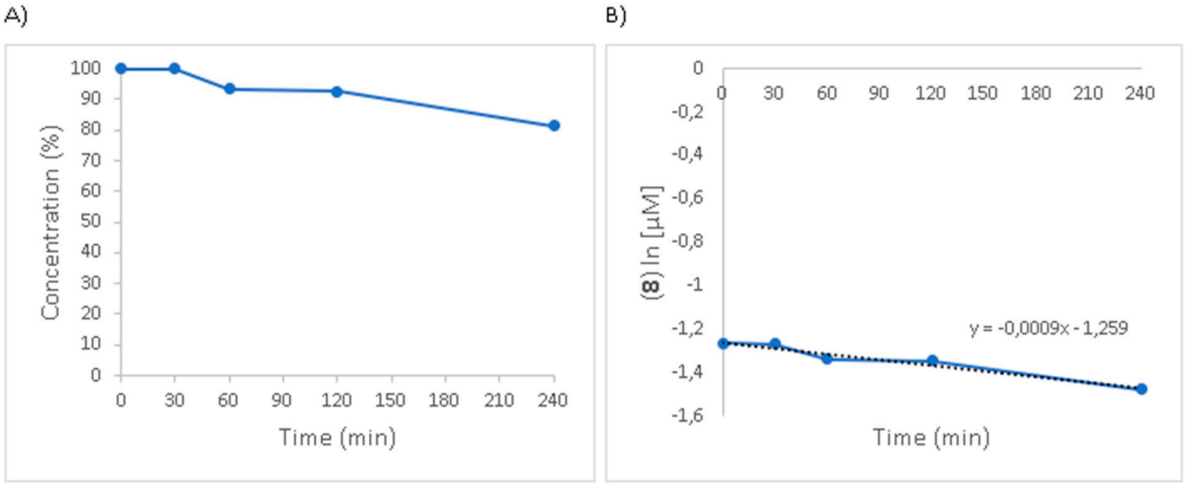

Figure S36. A) Plasma stability profile of (**8**); B) First order rate constant (k) for elimination.

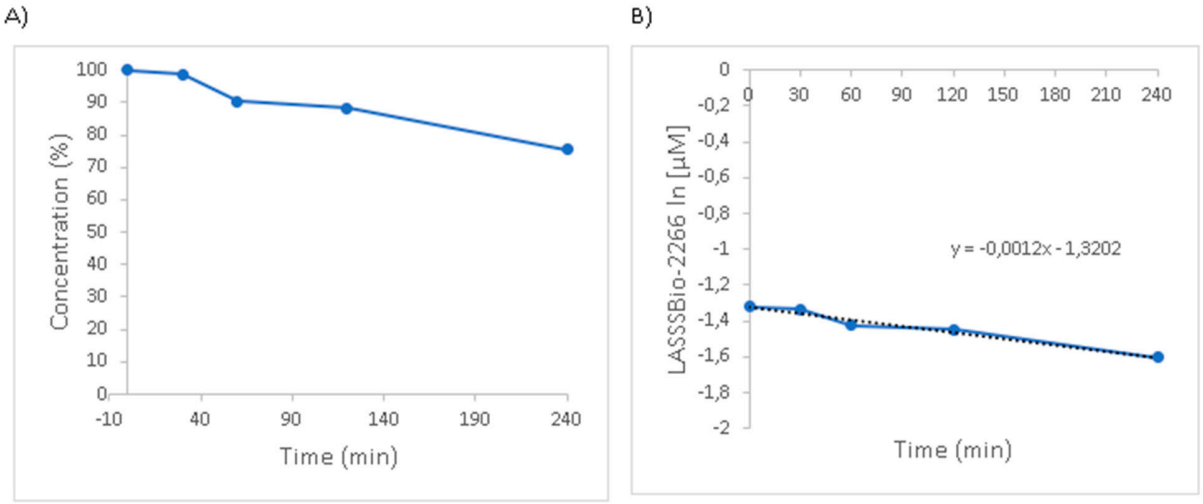

Figure S37. A) Plasma stability profile of (**9**); B) First order rate constant (k) for elimination.

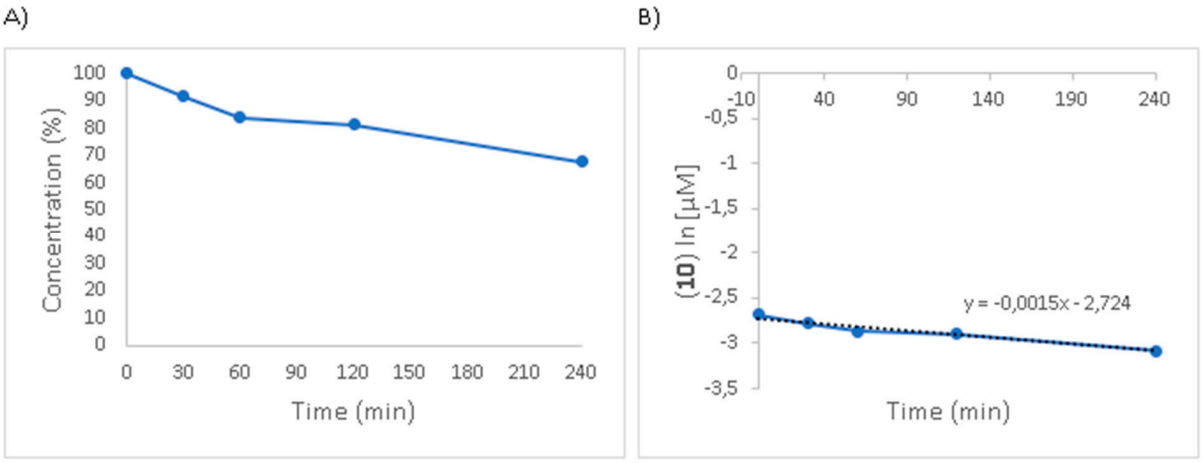

Figure S38. A) Plasma stability profile of (**10**); B) First order rate constant (k) for elimination.

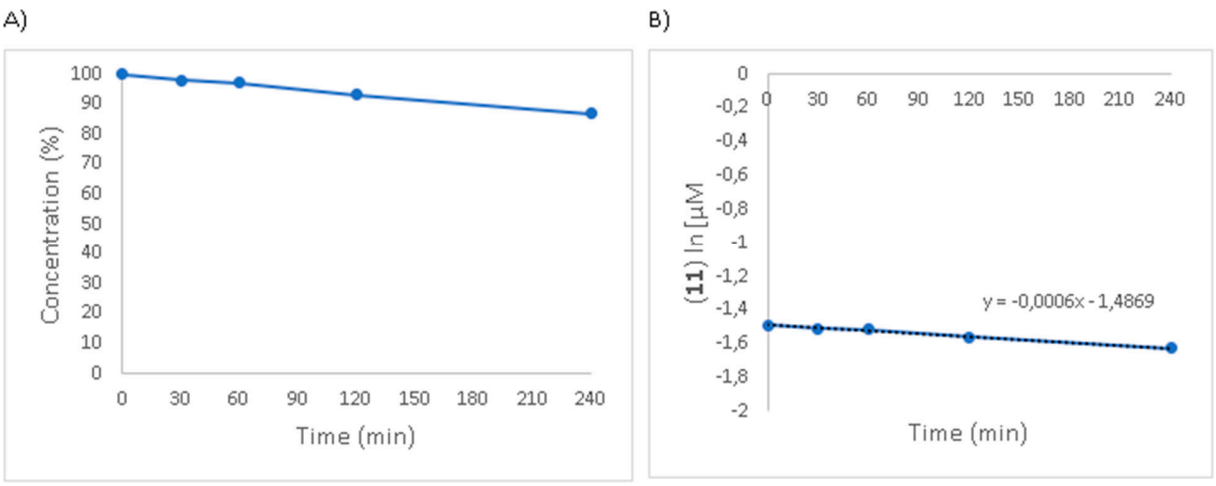

Figure S39. A) Plasma stability profile of (**11**); B) First order rate constant (k) for elimination.

Table S3. Evaluation the agonist effect against the CB1 receptors of the pyrazolamides (**7-11**).

Compound	% of control agonist* response activity at 1 μM	% of control agonist* response activity at 10 μM
(**7**)	10.4	25.3
(**8**)	6.5	14.4
(**9**)	16.9	23.6
(**10**)	12.5	26.1
(**11**)	6.7	4.6
* The control agonist used in the evaluation of agonist activity in CB1 cannabinoid receptors was CP 55,940 (EC_{50} = 3.3E-11 M)		

Table S4. Evaluation the agonist effect against the CB2 receptors of the pyrazolamides (**7-11**).

Compound	% of control agonis* response activity at 1 μM	% of control agonist* response activity at 10 μM
(**7**)	0.2	-78.1
(**8**)	-12.8	-157.8
(**9**)	-1.1	-41.5
(**10**)	-18.6	-102.8
(**11**)	-69.8	-119.6
* The control agonist used in the evaluation of agonist activity in CB2 cannabinoid receptors was WIN 55212-2 (EC50 = 2.4E-10 M)		

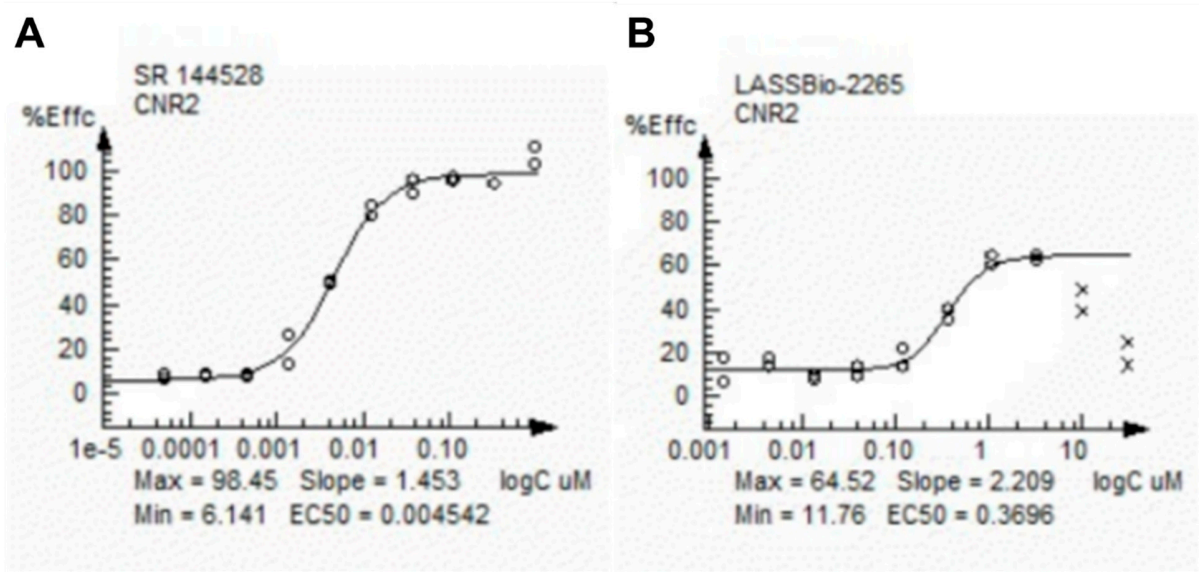

Figure S40. Dose-response curve of inverse agonism for cannabinoid receptor 2 (CB2) performed by the company Eurofins-CEREP: (**A**) control inverse agonist SR 144528 and (**B**) LASSBio-2265 (**11**).

Table S5. Raw data from the inverse agonism assay performed by the company Eurofins-CEREP

Compound Name	Assay Format	RC50	Unit	Hill	Curve Bottom	Curve Top	Max Response
CP55940	Agonist	0.001022727	uM	1.3517	-5.1253	100	102.06
SR 144528	Inverse Agonist	0.004542448	uM	1.4529	6.1415	98.455	106.31
LASSBio-2265	Inverse Agonist	0.3695975	uM	2.209	11.761	64.52	63.063